Astro/Phys 224   Spring 2012
Origin and Evolution of the Universe

Week 5

CMB and Structure Formation

Joel Primack
**University of California, Santa Cruz**

Cosmic Microwave Background

Early History

Although Penzias and Wilson discovered the CMB in 1965, Weinberg (p. 104) points out that Adams and McKellar had shown that the rotational spectra of cyanogen (CN) molecules observed in 1941 suggested that the background temperature is about 3K.

The COBE FIRAS measurements showed that the spectrum is that of thermal radiation with T = 2.73K. John Mather, the FIRAS PI, shared the 2006 Nobel Prize with George Smoot, the COBE/DMR PI.

The earth's motion (including that of the sun and the Milky Way) produces a CMB dipole anisotropy.

CMB dipole
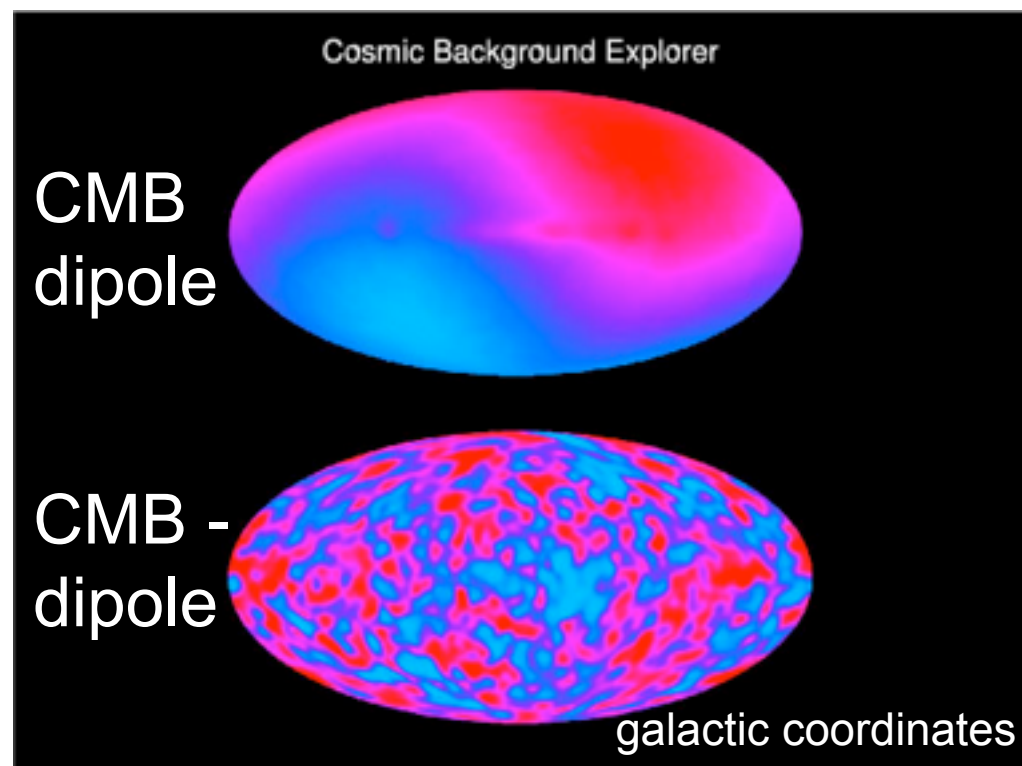
CMB - dipole

The CMB dipole anisotropy was discovered by Paul Henry (1971) and Edward Conklin (1972), and confirmed by Conklin and Wilkinson (1977) and Smoot, Gorenstein, and Muller (1977) -- see http://www.astro.ucla.edu/~wright/CMB-dipole-history.html

The upper panel of the figure shows the CMB dipole anisotropy in the COBE data. It is usually subtracted when the temperature anisotropy map is displayed (lower panel).

CMB Temperature Anisotropy

Sachs & Wolfe (1967, ApJ, 147, 73) showed that on large angular scales the temperature anisotropy is $\Delta T/T = \varphi/3c^2$. White & Hu give a pedagogical derivation in http://background.uchicago.edu/~whu/Papers/sw.pdf

PERTURBATIONS OF A COSMOLOGICAL MODEL AND ANGULAR VARIATIONS OF THE MICROWAVE BACKGROUND

R. K. SACHS AND A. M. WOLFE

Relativity Center, The University of Texas, Austin, Texas

ABSTRACT

We consider general-relativistic, spatially homogeneous, and isotropic $k = 0$ cosmological models with either pressure zero or pressure one-third the energy density. The equations for general linearized perturbations away from these models are explicitly integrated to obtain density fluctuations, rotational perturbations, and gravitational waves. The equations for light rays in the perturbed models are integrated. The models are used to estimate the anisotropy of the microwave radiation, assuming this radiation is cosmological. It is estimated that density fluctuations now of order 10 per cent with characteristic lengths now of order 1000 Mpc would cause anisotropies of order 1 per cent in the observed microwave temperature due to the gravitational redshift and other general-relativistic effects. The $p = 0$ models are compared in detail with corresponding Newtonian models. The perturbed Newtonian models do not contain gravitational waves, but the density perturbations and rotational perturbations are surprisingly similar.

This was first convincingly seen by the COBE DMR experiment, reported by George Smoot on April 27, 1992. Their result $\Delta T/T = 10^{-5}$ had been predicted by the CDM model (Blumenthal, Faber, Primack, & Rees 1984). The search then began for smaller-angular-scale CMB anisotropies.

Shown at DM2000:

Shown at DM2002:

Max Tegmark

Shown at DM2004:

WMAP

Shown at DM2006:

THE COSMIC SYMPHONY

By Wayne Hu and Martin White

New observations of the cosmic microwave background radiation show that the early universe resounded with harmonious oscillations
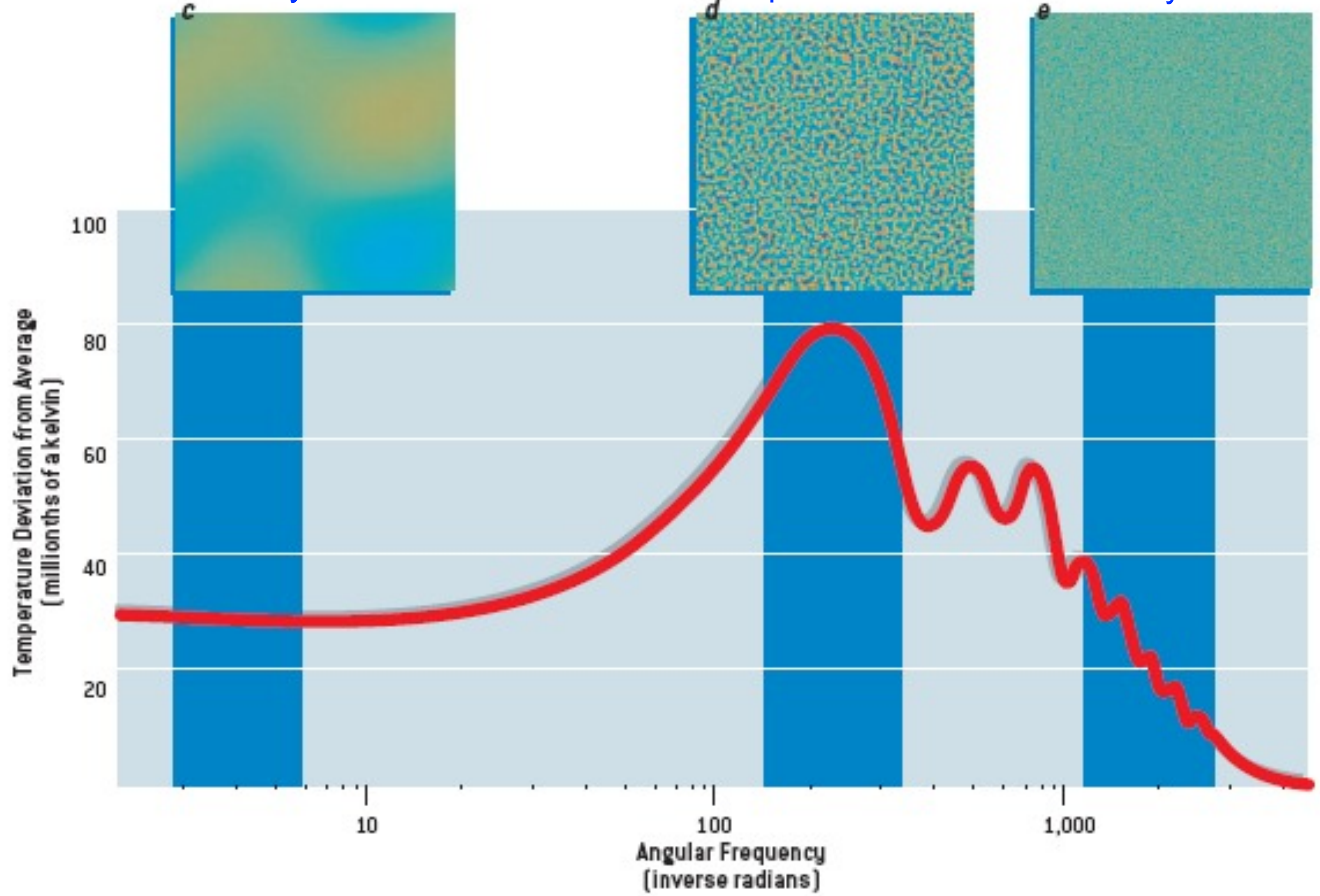
Scientific American   February 2004

Angular Thermal Variations

GRAVITATIONAL MODULATION

INFLUENCE OF DARK MATTER modulates the acoustic signals in the CMB. After inflation, denser regions of dark matter that have the same scale as the fundamental wave (*represented as troughs in this potential-energy diagram*) pull in baryons and photons by gravitational attraction. (The troughs are shown in red because gravity also reduces the temperature of any escaping photons.) By the time of recombination, about 380,000 years later, gravity and sonic motion have worked together to raise the radiation temperature in the troughs (*blue*) and lower the temperature at the peaks (*red*).
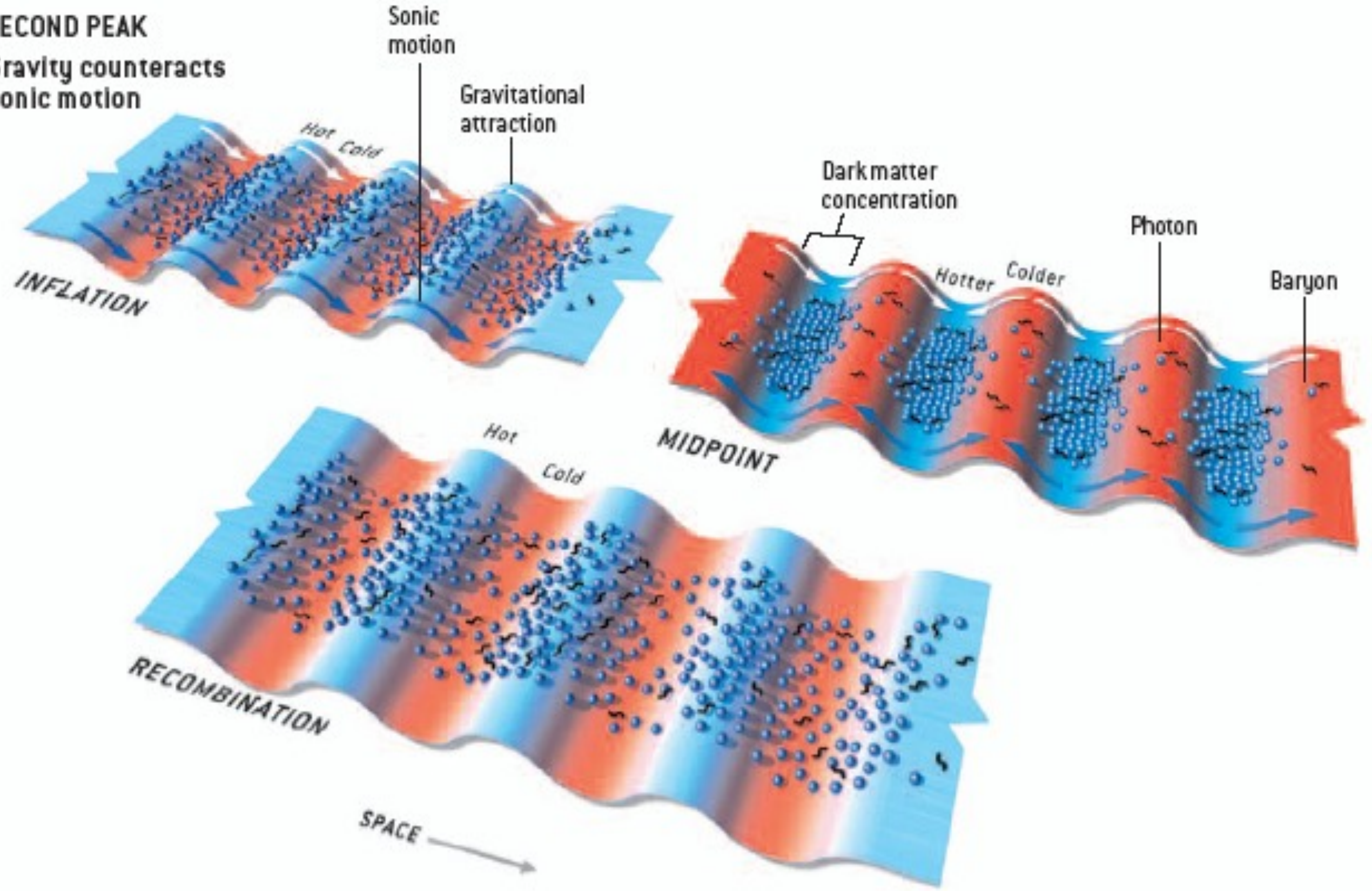
FIRST PEAK

Gravity and sonic motion work together

Thursday, May 3, 12
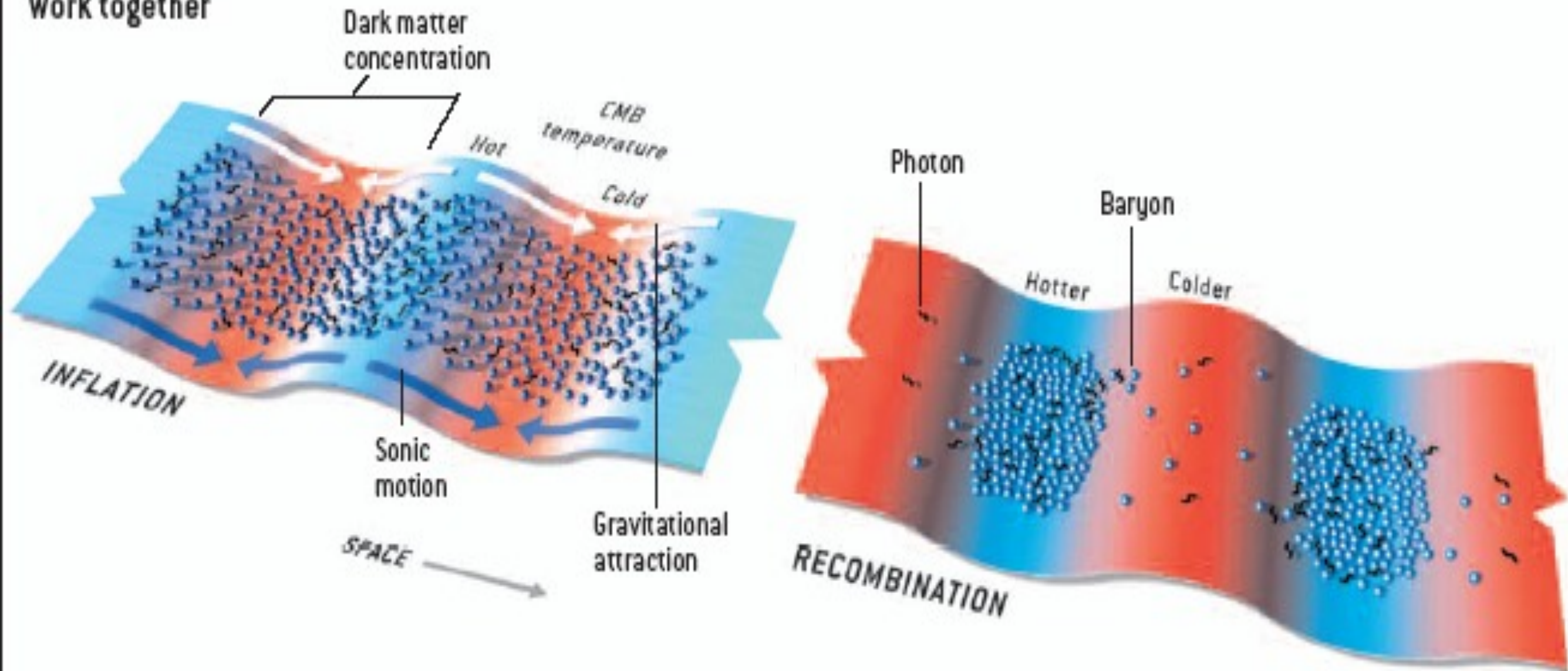
AT SMALLER SCALES, gravity and acoustic pressure sometimes end up at odds. Dark matter clumps corresponding to a second-peak wave maximize radiation temperature in the troughs long before recombination. After this midpoint, gas pressure pushes baryons and photons out of the troughs (*blue arrows*) while gravity tries to pull them back in (*white arrows*). This tug-of-war decreases the temperature differences, which explains why the second peak in the power spectrum is lower than the first.


SECOND PEAK
Gravity counteracts sonic motion

Sonic motion

Gravitational attraction

INFLATION

Hot Cold

Dark matter concentration

Hotter Colder

Photon

Baryon

MIDPOINT

Hot

Cold

RECOMBINATION

SPACE

Piper at the Gates of Dawn

- Blow into a flute or an open pipe

- Spectrum of sound contains a fundamental frequency and harmonic overtones

mouthpiece

fundamental

1st overtone

2nd overtone

3rd overtone
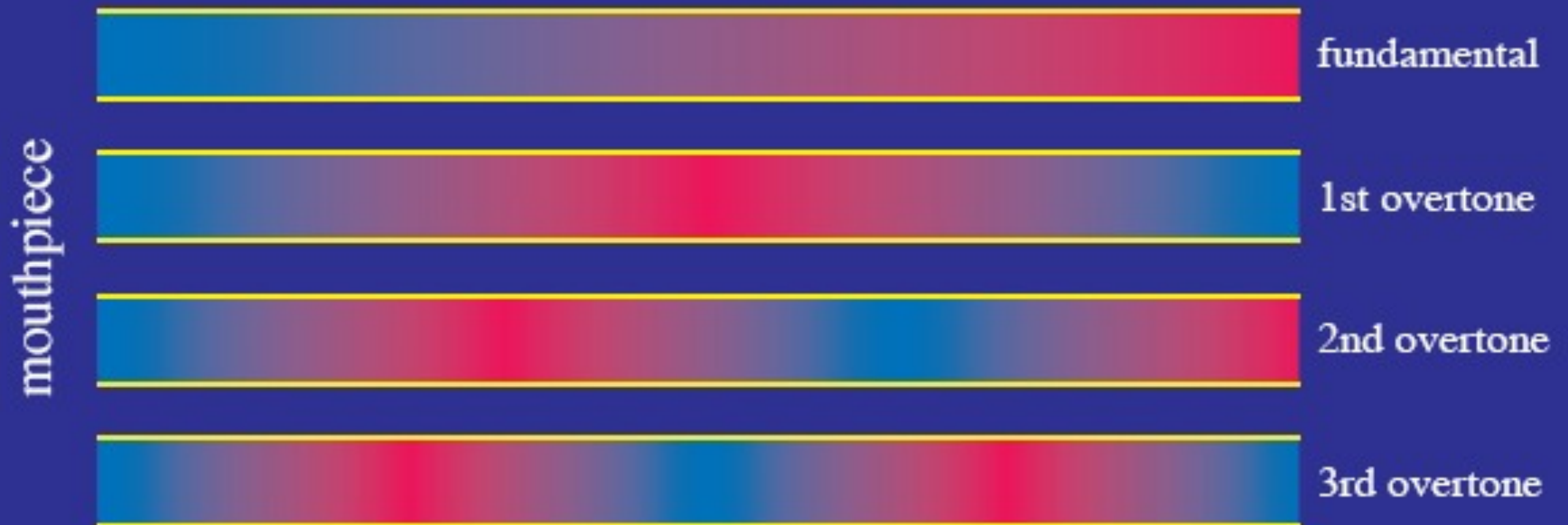
This and the next several slides are from a talk by Wayne Hu; see
http://background.uchicago.edu/~whu/beginners/introduction.html

Piper at the Gates of Dawn

- Inflation is the source of sound waves at the beginning of time

- Sound waves are frozen at recombination, yielding a harmonic spectrum of frequencies that reach maximum displacement
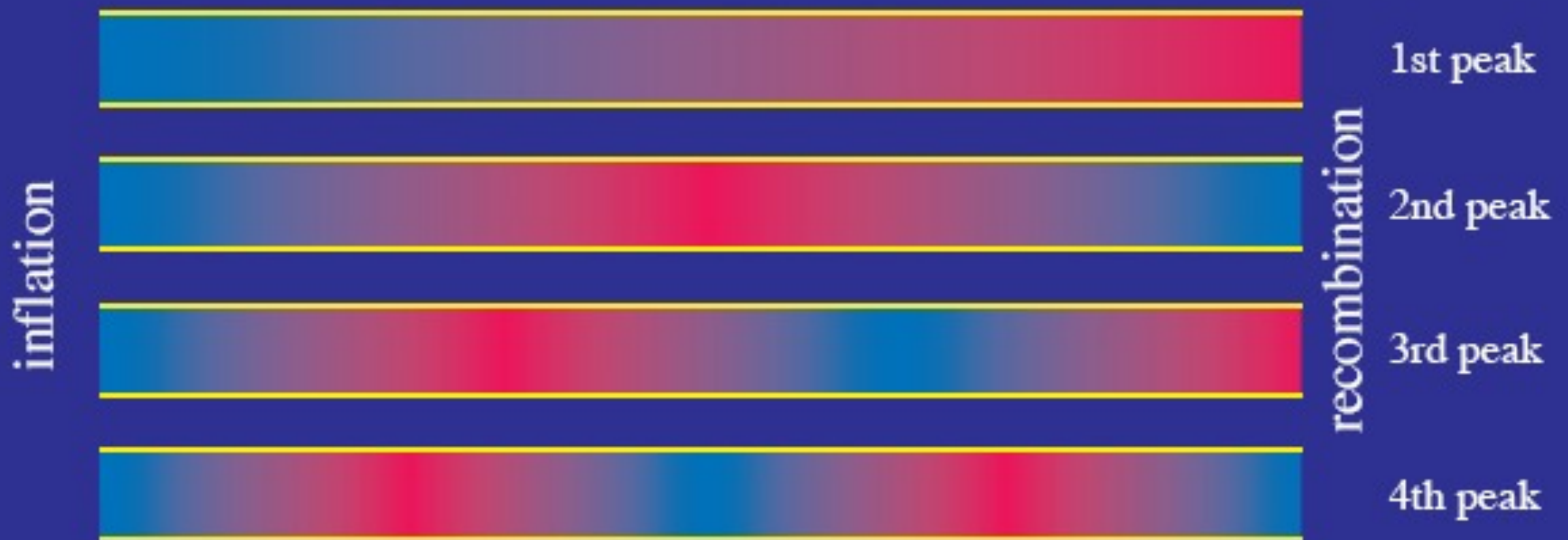
See also Annual Rev. Astron. and Astrophys. 2002
Cosmic Microwave Background Anisotropies
by Wayne Hu and Scott Dodelson

Harmonic Signature

- Much like a musical instrument, identify construction through the pattern of overtones on the fundamental frequency

- Without inflation, fluctuations must be generated at intermediate times

- Like drilling holes in the pipe and blowing in random places, harmonic structure of peaks destroyed

- Observed frequency spectrum consistent with inflationary origin

- Detailed examination of the overtones, reveals the composition of the universe

- But first...

Fundamental: Weighing the Universe

- Measuring the angular extent of the fundamental wavelength (spot size) yields the curvature - universe is spatially flat

- Einstein says matter-energy density curves space: universe is at the critical density


Flat

Closed
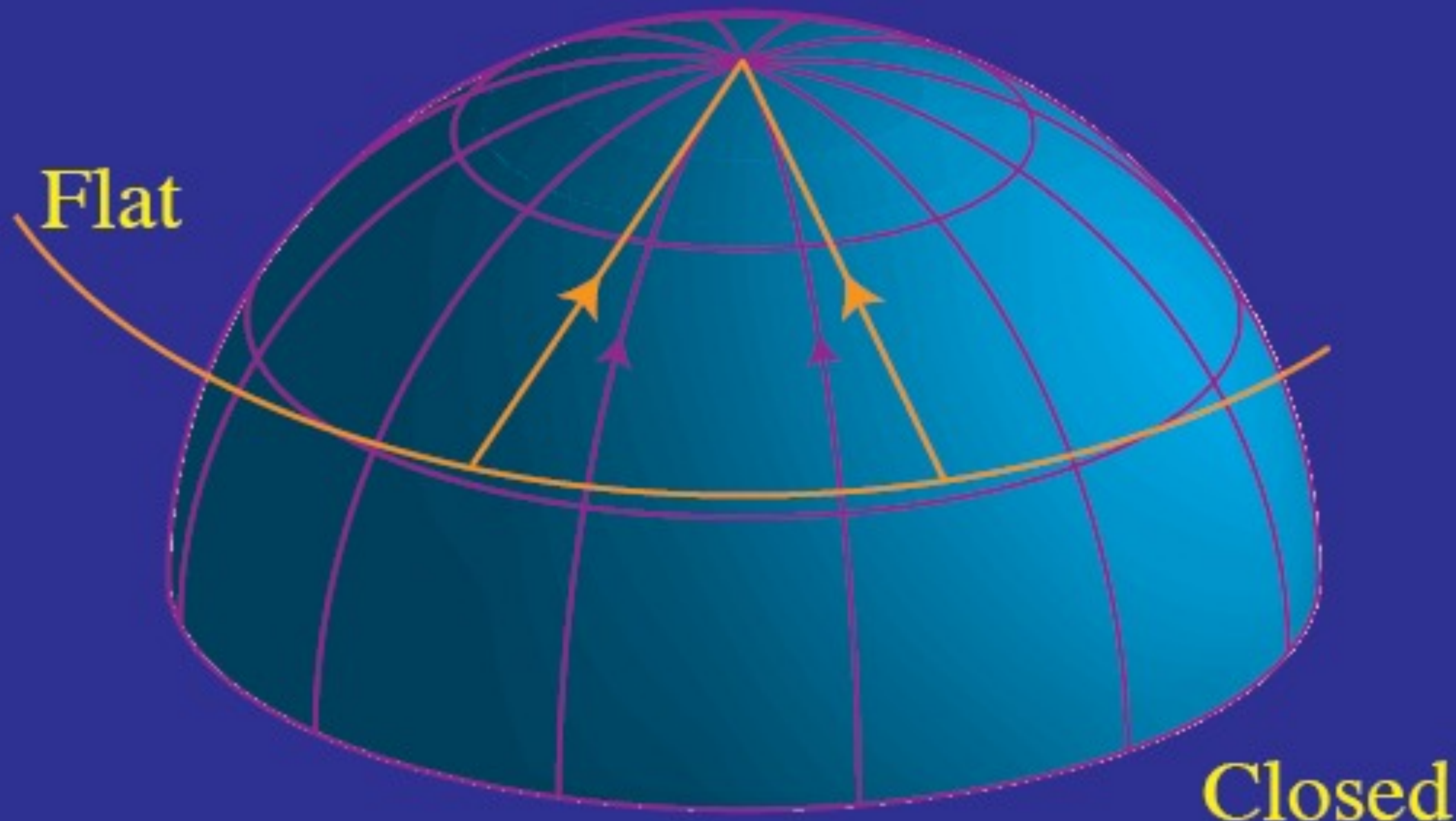
Sound Spectrum

- Spectrum of sound shows harmonics at integer ratios of the fundamental
- Other models that generate structure causally at intermediate times would not have these harmonics
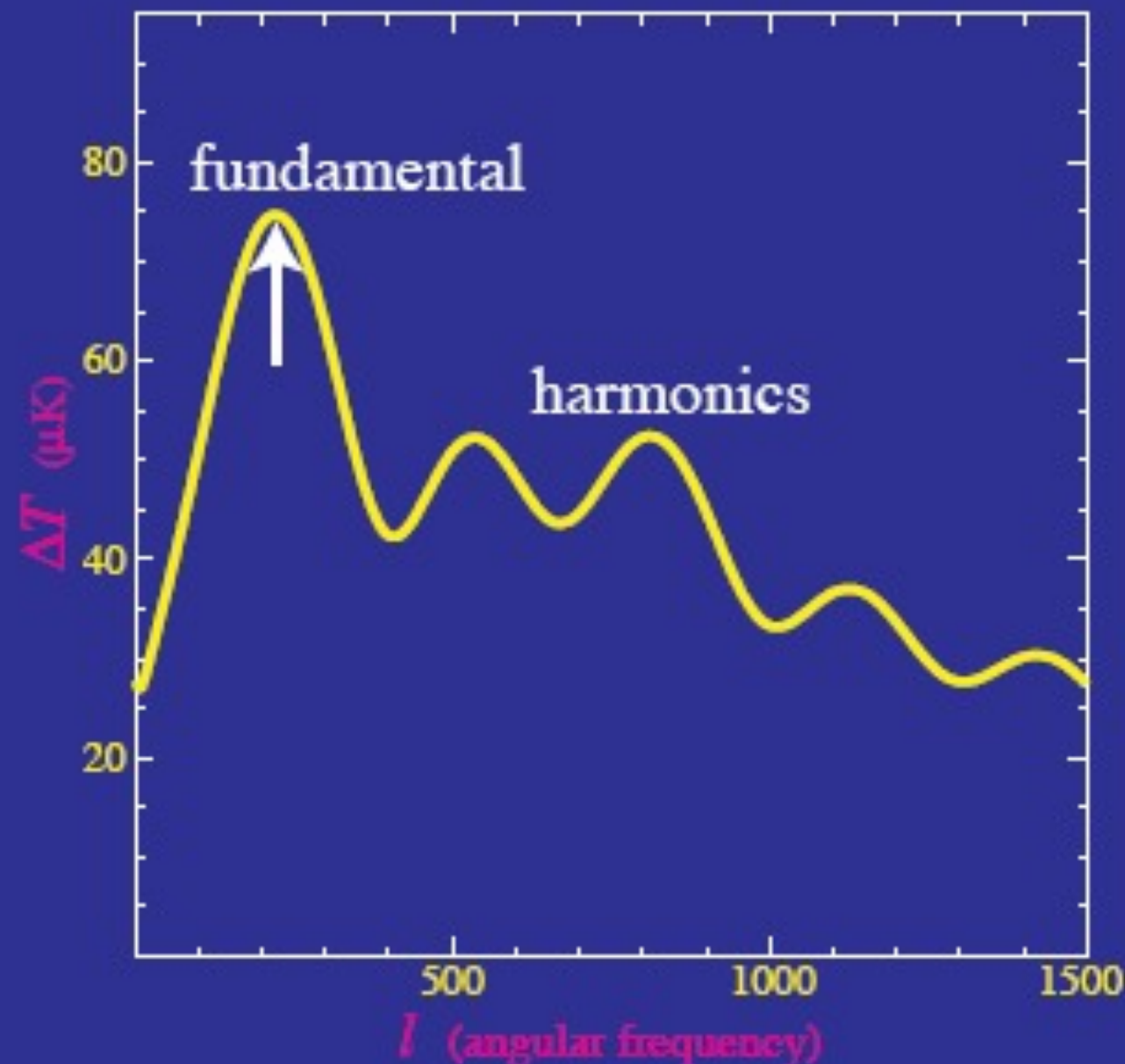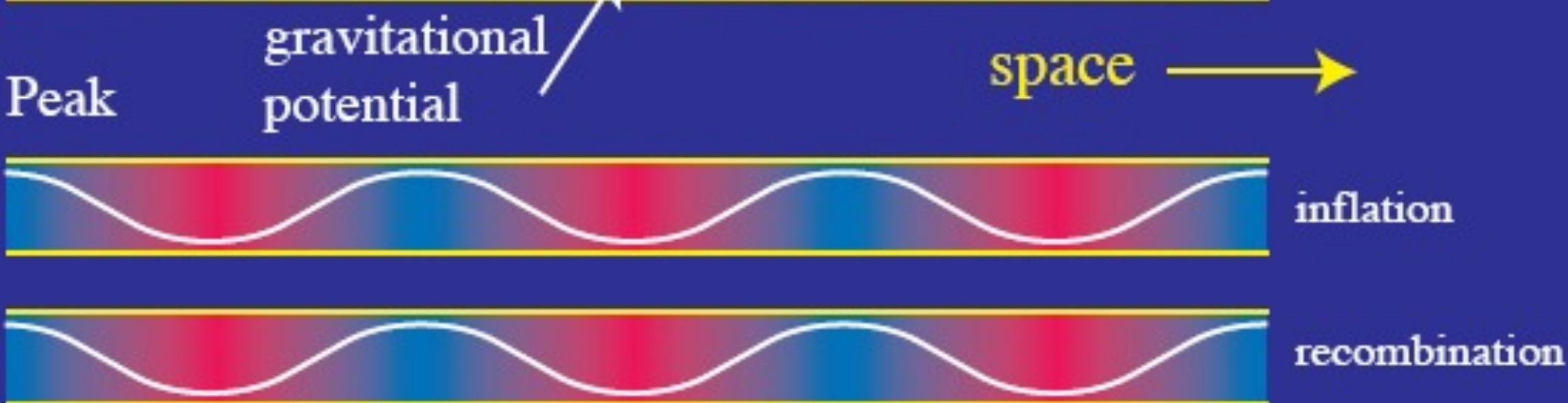
Harmonics: Ordinary Matter

- Competition between gravity and pressure depends on phase of oscillation

- At the fundamental (and odd frequency multiples) gravity assists sonic motion; at second peak (and even multiples) gravity fights sonic motion

Fundamental

inflation

recombination

gravitational potential

space

2nd Peak

inflation

recombination
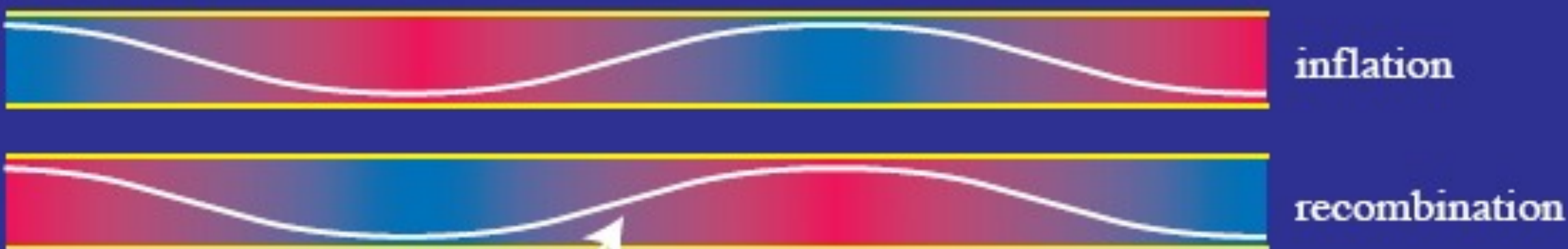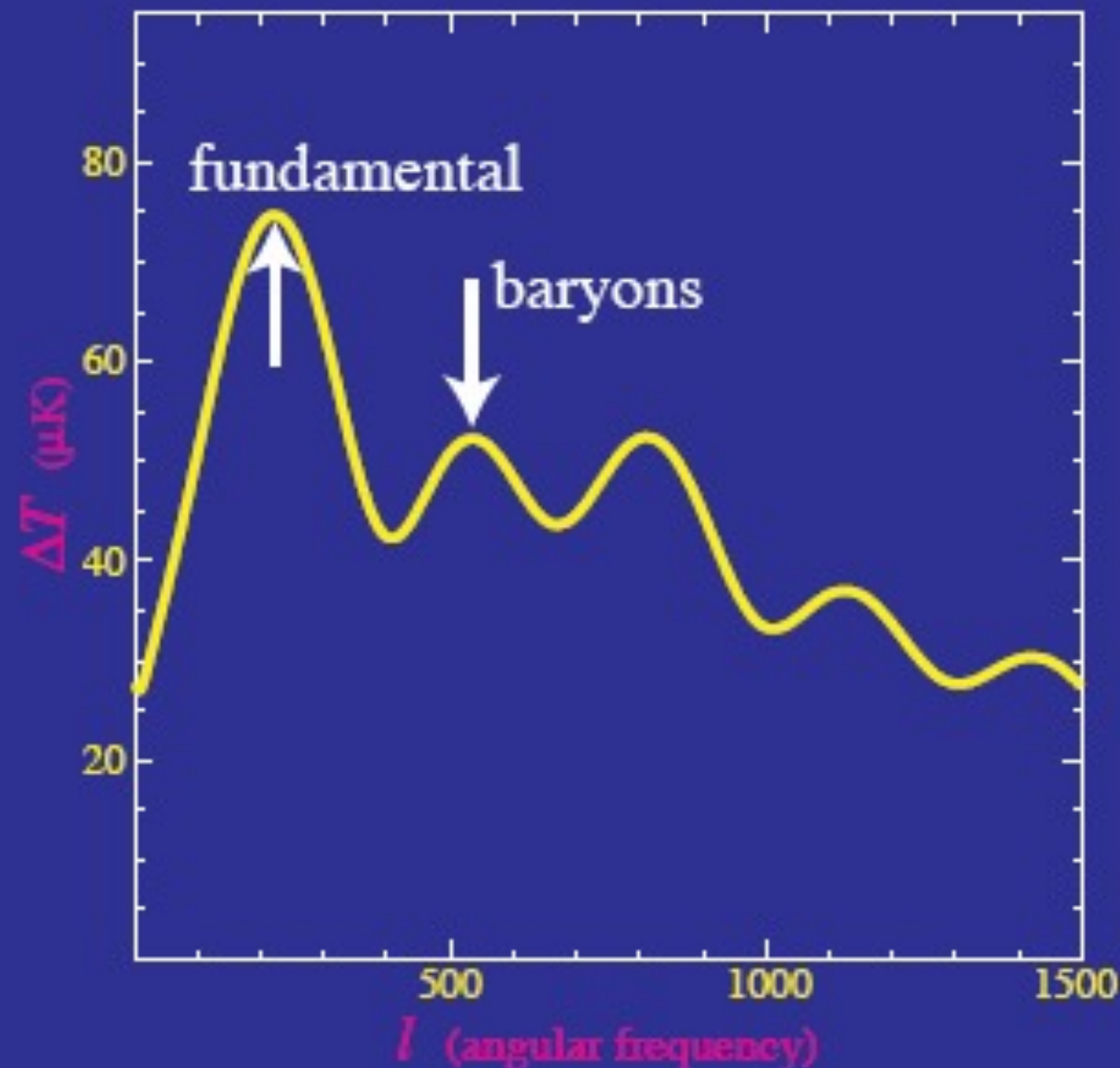
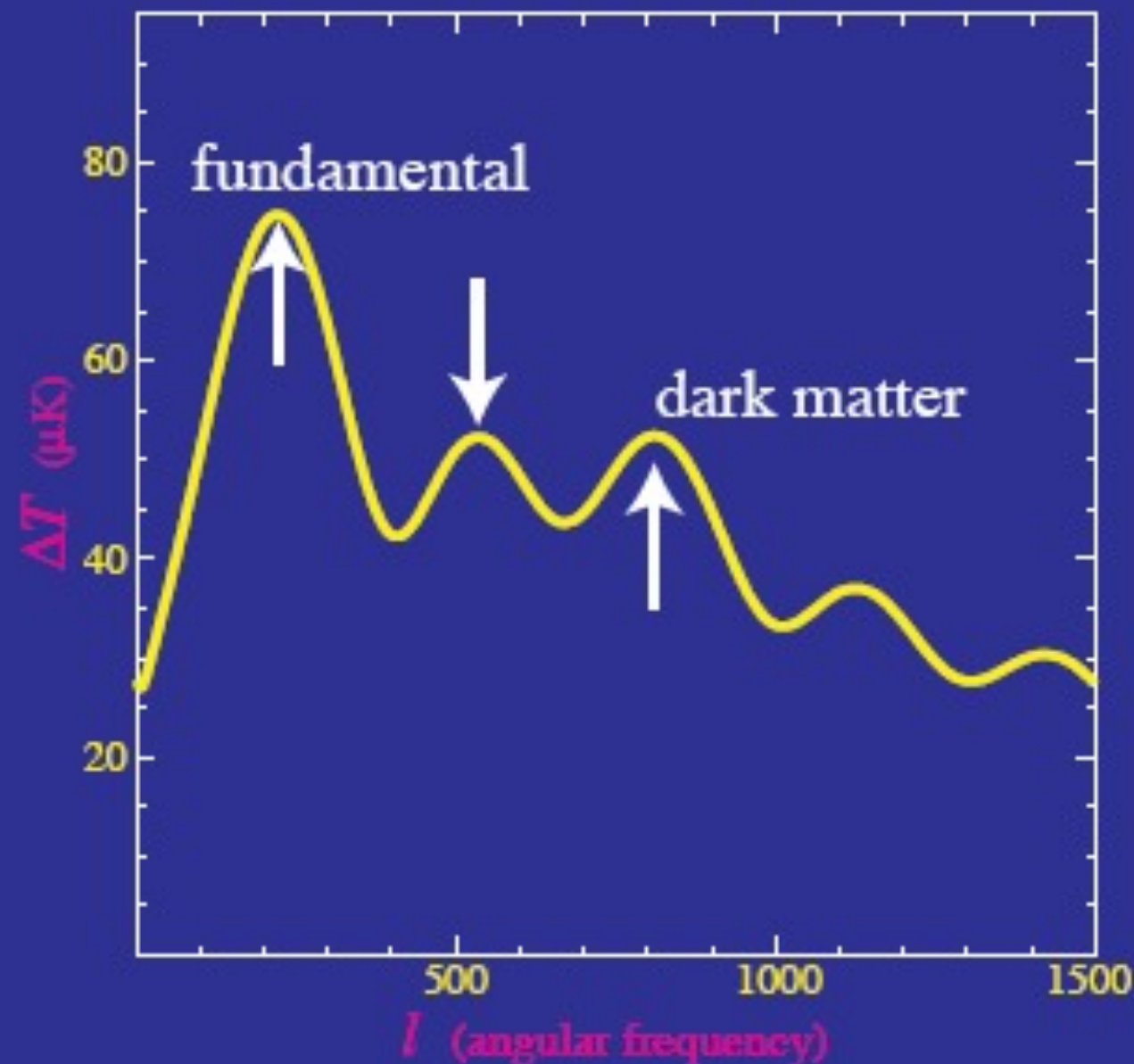# Ordinary Matter

- A low second peak indicates baryon or ordinary matter density comparable to photon density

- Ordinary matter consists of ~5% of the critical density today

Dark Matter

- A third peak comparable to second peak indicates a dark matter density ~5x that of ordinary matter

- Dark matter ~25% of the critical density

Gravitational Ringing

- Potential wells = inflationary seeds of structure
- Fluid falls into wells, pressure resists: acoustic oscillations

Gravity

Pressure

Extrema=Peaks

- First peak = mode that just compresses
- Second peak = mode that compresses then rarefies: twice the wavenumber
- Harmonic peaks: 1:2:3 in wavenumber

Recombination — First Peak — time — $k_1 = \pi/\text{sound horizon}$ — $-|\Psi|/3$

Recombination — Second Peak — time — $k_2 = 2k_1$ — $-|\Psi|/3$

From Wayne Hu's Warner Prize Lecture, AAS meeting Jan 2001

http://background.uchicago.edu/~whu/Presentations/warnerprint.pdf

1st compression

2nd compression

Maxima

1st rarefaction

damping

$\Delta T\,(\mu K)$

l

W. Hu 11/00

Predictive Power

- Model **predicts** the precise form of the **damping** of sound waves: observed ✔

- Model **predicts** that associated with the damping, the CMB becomes polarized: observed ✔

- Model **predicts** that temperature fluctuations **correlated** with local structure due to the **dark energy**: observed ✔
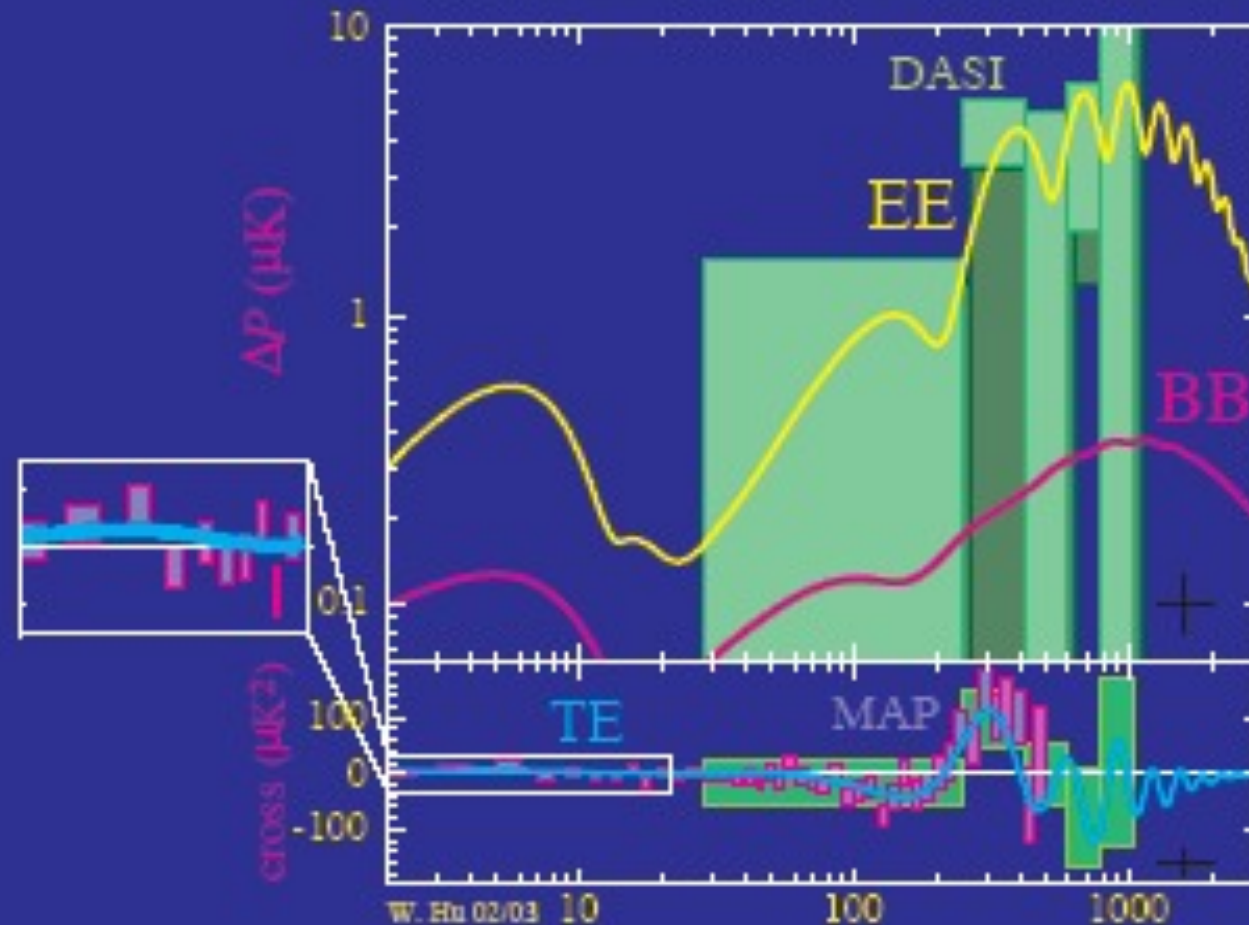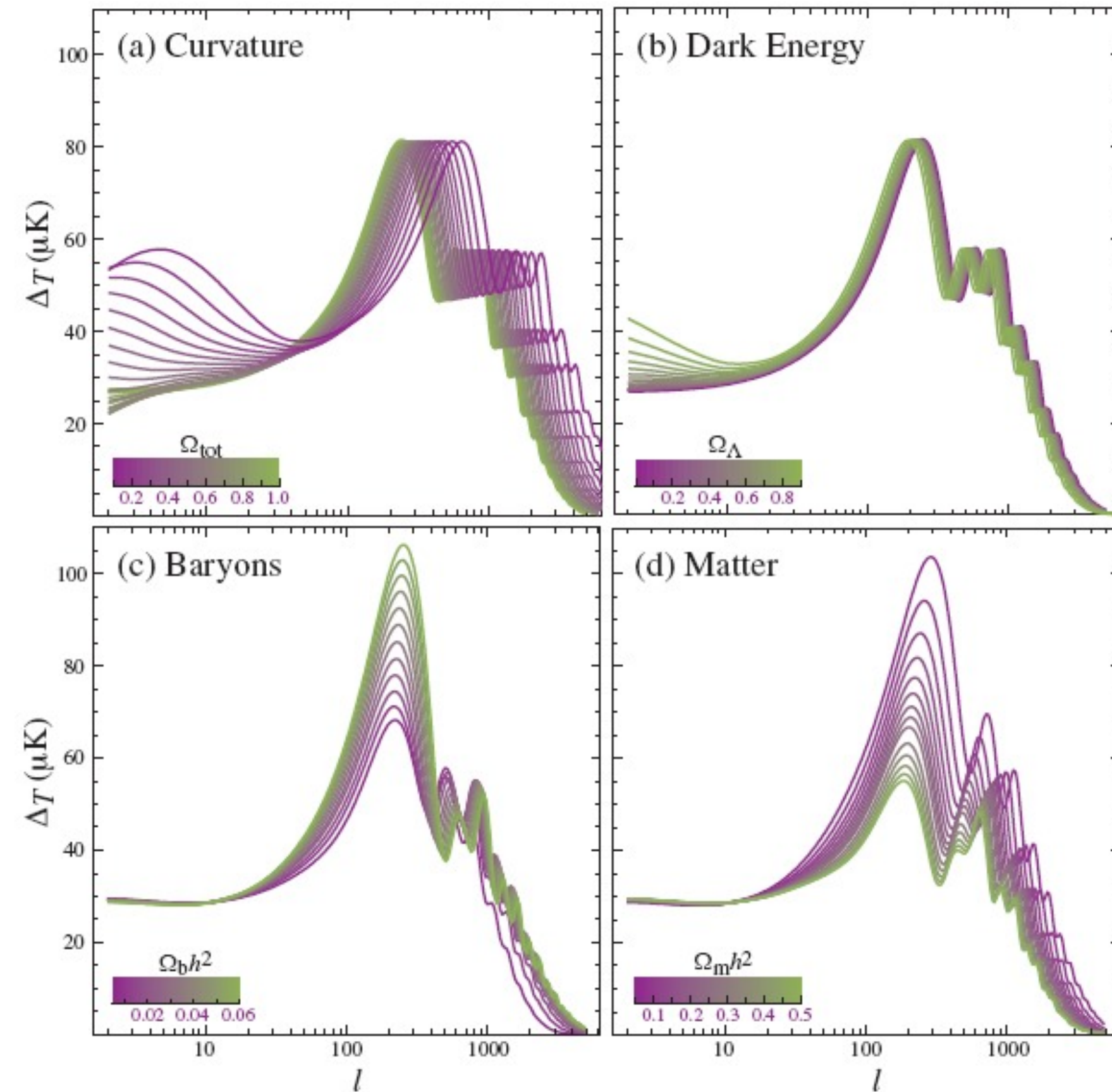
Plate 4: Sensitivity of the acoustic temperature spectrum to four fundamental cosmological parameters (a) the curvature as quantified by Ω_{tot} (b) the dark energy as quantified by the cosmological constant Ω_Λ ($w_\Lambda = -1$) (c) the physical baryon density $\Omega_b h^2$ (d) the physical matter density $\Omega_m h^2$, all varied around a fiducial model of $\Omega_{tot} = 1$, $\Omega_\Lambda = 0.65$, $\Omega_b h^2 = 0.02$, $\Omega_m h^2 = 0.147$, $n = 1$, $z_{ri} = 0$, $E_i = 0$.

Annu. Rev. Astron. and Astrophys. 2002
Cosmic Microwave Background Anisotropies by **Wayne Hu** and **Scott Dodelson**

For animation of the effects of changes in cosmological parameters on the CMB angular power spectrum and the matter power spectrum, plus links to many CMB websites, see Max Tegmark's and Wayne Hu's websites:

http://space.mit.edu/home/tegmark/

http://background.uchicago.edu/~whu/physics/physics.html

Five-Year Wilkinson Microwave Anisotropy Probe (WMAP[1]) Observations:
Data Processing, Sky Maps, & Basic Results

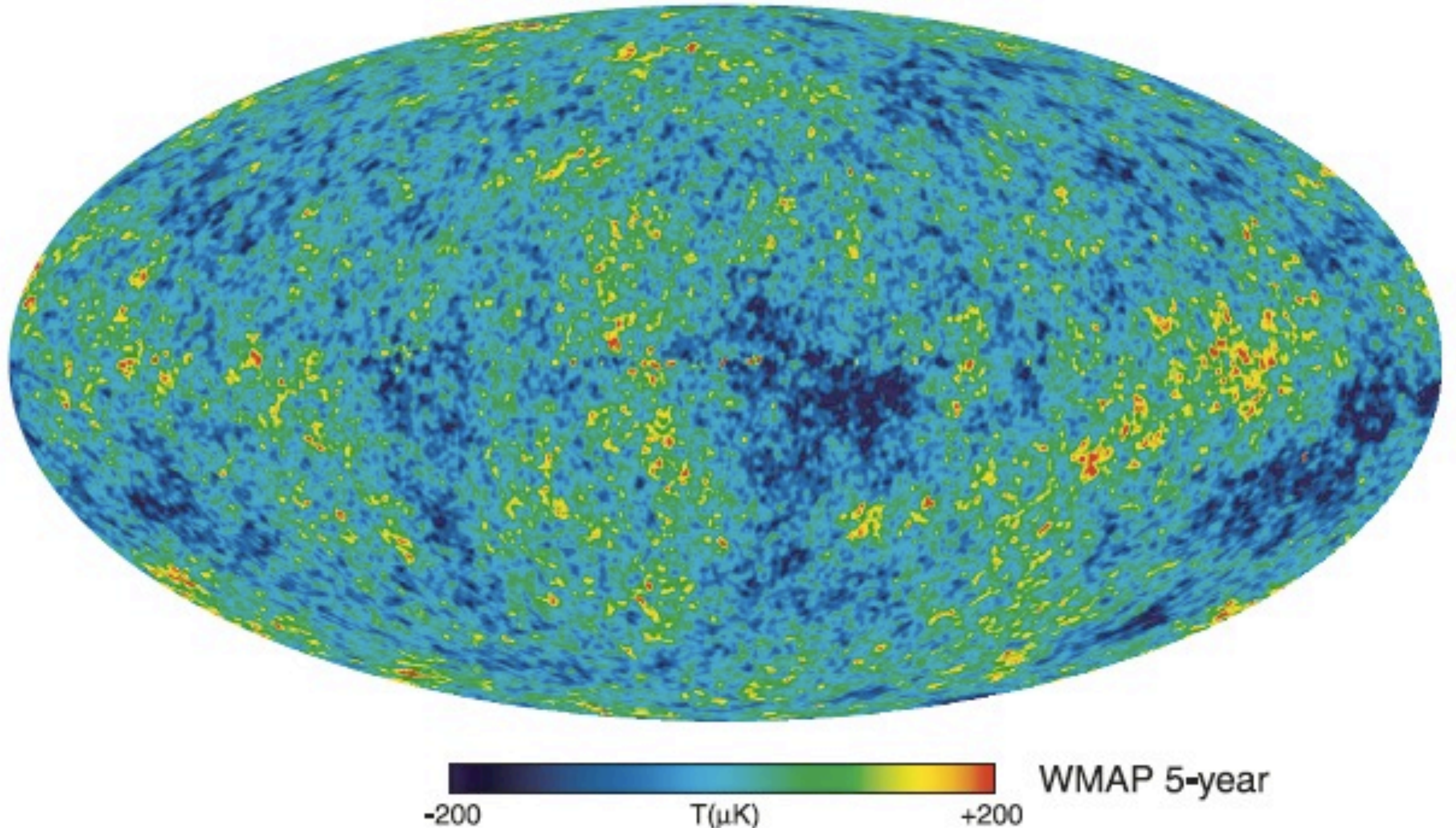
-200   T(μK)   +200   WMAP 5-year

Fig. 12. The foreground-reduced Internal Linear Combination (ILC) map.

J. Dunkley, et.al. Five-Year Wilkinson Microwave Anisotropy Probe (WMAP) Observations: Likelihoods and Parameters from WMAP Data (2008)

Final paragraph of Conclusions:

Considering a range of extended models, we continue to find that **the standard ΛCDM model is consistently preferred by the data**. The improved measurement of the third peak now requires the existence of light relativistic species, assumed to be neutrinos, at high confidence. The standard scenario has three neutrino species, but the three-year WMAP data could not rule out models with none. **The CDM model also continues to succeed in fitting a substantial array of other observations.** Certain tensions between other observations and those of WMAP, such as the amplitude of matter fluctuations measured by weak lensing surveys and using the Ly-α forest, and the primordial lithium abundance, have either been resolved with improved understanding of systematics, or show promise of being explained by recent observations. With further WMAP observations we will better probe both the universe at a range of epochs, measuring fluctuation characteristics to probe the initial inflationary process, or other non-inflationary scenario, improving measurements of the composition of the universe at the recombination era, and characterizing the reionization process in the universe.

The WMAP 7-Year Internal Linear Combination Map is a weighted linear combination of the five WMAP frequency maps. The weights are computed using criteria which minimize the Galactic foreground contribution to the sky signal. The resultant map provides a low-contamination image of the CMB anisotropy.
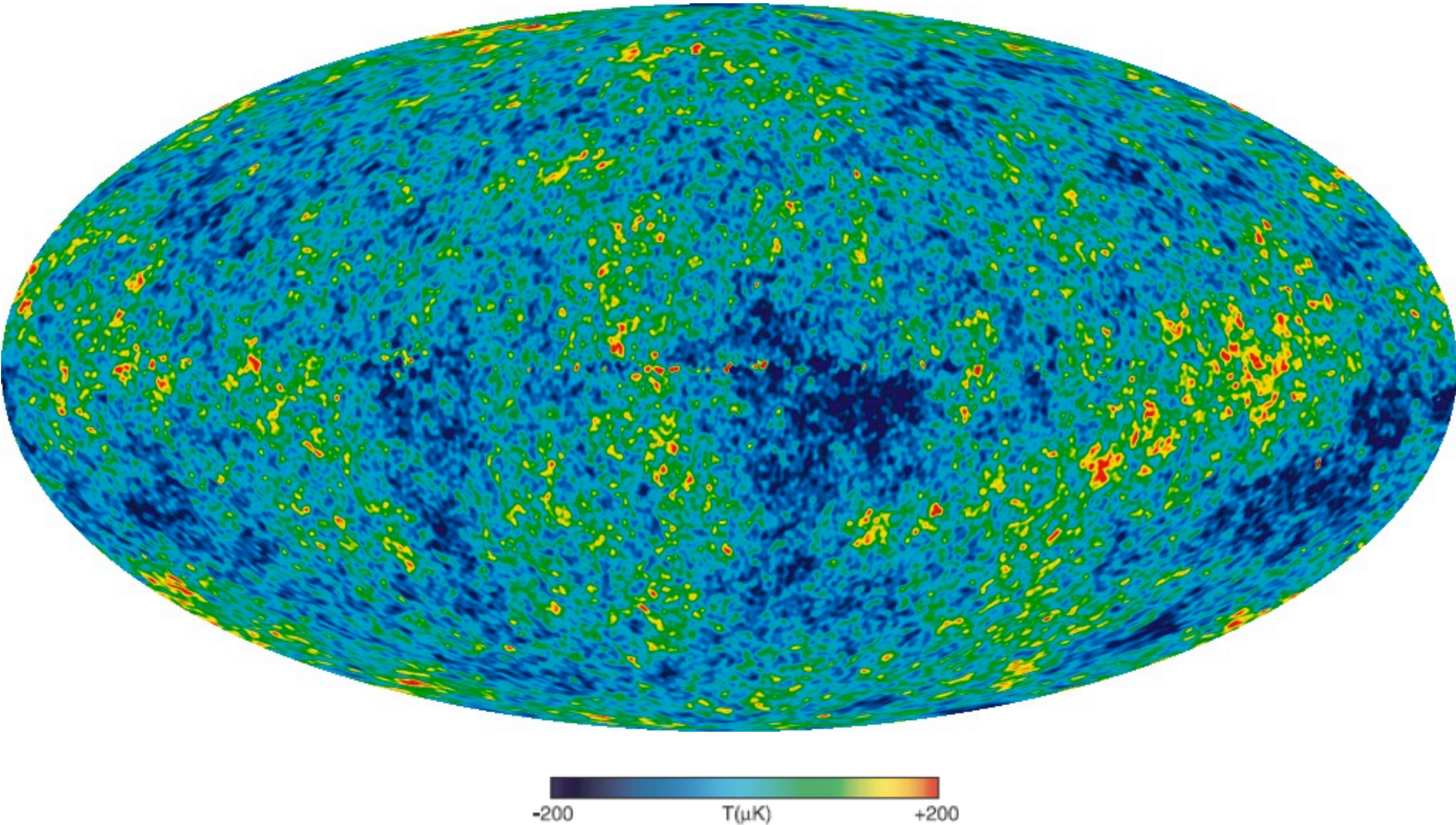
-200   T(µK)   +200

http://lambda.gsfc.nasa.gov/product/space/

Seven-Year Wilkinson Microwave Anisotropy Probe (WMAP) Observations:
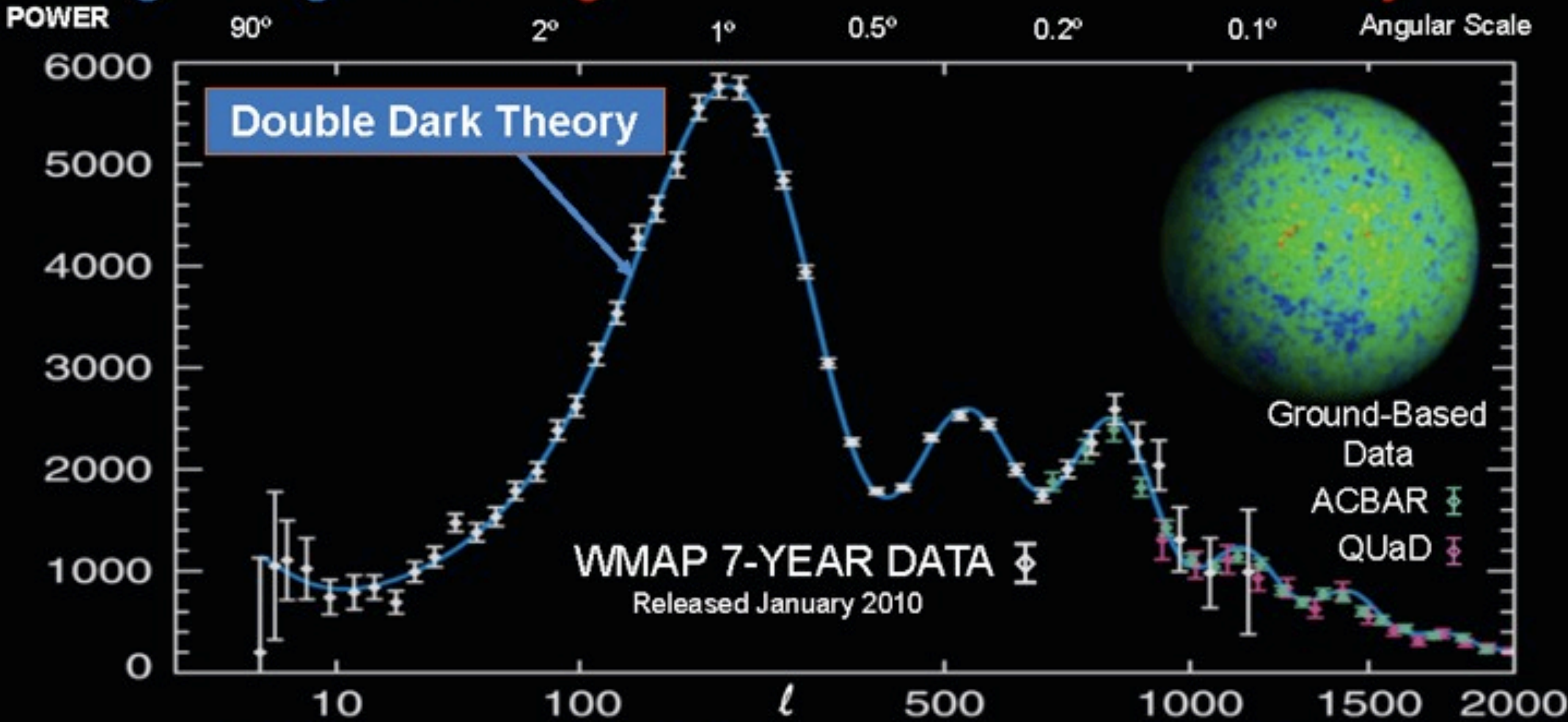Sky Maps, Systematic Errors, and Basic Results - N. Jarosik et al. - January 2010

The seven year data set is well fit by a minimal six-parameter flat ΛCDM model. The parameters for this model, using the WMAP data in conjunction with baryon acoustic oscillation data from the Sloan Digital Sky Survey and priors on H_0 from Hubble Space Telescope observations, are: $\Omega_b h^2 = 0.02260 \pm 0.00053$, $\Omega_c h^2 = 0.1123 \pm 0.0035$, $\Omega_\Lambda = 0.728^{+0.015}_{-0.016}$, $n_s = 0.963 \pm 0.012$, $\tau = 0.087 \pm 0.014$ and $\sigma_8 = 0.809 \pm 0.024$ (68 % CL uncertainties).

The temperature power spectrum signal-to-noise ratio per multipole is greater that unity for multipoles $\ell \lesssim 919$, allowing a robust measurement of the third acoustic peak. This measurement results in improved constraints on the matter density, $\Omega_m h^2 = 0.1334^{+0.0056}_{-0.0055}$, and the epoch of matter-radiation equality, $z_{eq} = 3196^{+134}_{-133}$, using WMAP data alone.

The new WMAP data, when combined with smaller angular scale microwave background anisotropy data, results in a 3σ detection of the abundance of primordial Helium, $Y_{He} = 0.326 \pm 0.075$. When combined with additional external data sets, the WMAP data also yield better determinations of the total mass of neutrinos, $\sum m_\nu = < 0.58$ eV (95% CL), and the effective number of neutrino species, $N_{eff} = 4.34^{+0.86}_{-0.88}$. The power-law index of the primordial power spectrum is now determined to be $n_s = 0.963 \pm 0.012$, excluding the Harrison-Zel'dovich-Peebles spectrum by $> 3\sigma$

These new WMAP measurements provide important tests of Big Bang cosmology.

Big Bang Data Agrees with Double Dark Theory!

Double Dark Theory

WMAP 7-YEAR DATA
Released January 2010

Ground-Based Data
ACBAR
QUaD

Cosmic Background Explorer COBE 1992
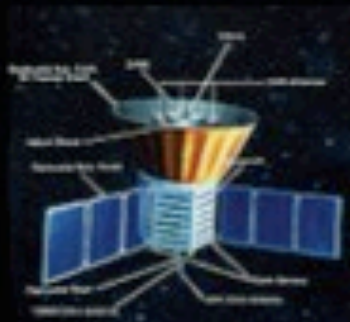
Wilkinson Microwave Anisotropy Probe WMAP 2003-

ACBAR

QUaD

Thursday, May 3, 12

http://lambda.gsfc.nasa.gov/product/space/

Seven-Year Wilkinson Microwave Anisotropy Probe (WMAP) Observations:
Sky Maps, Systematic Errors, and Basic Results - N. Jarosik et al. - January 2010

1st peak at 1^0
⇒ space is flat

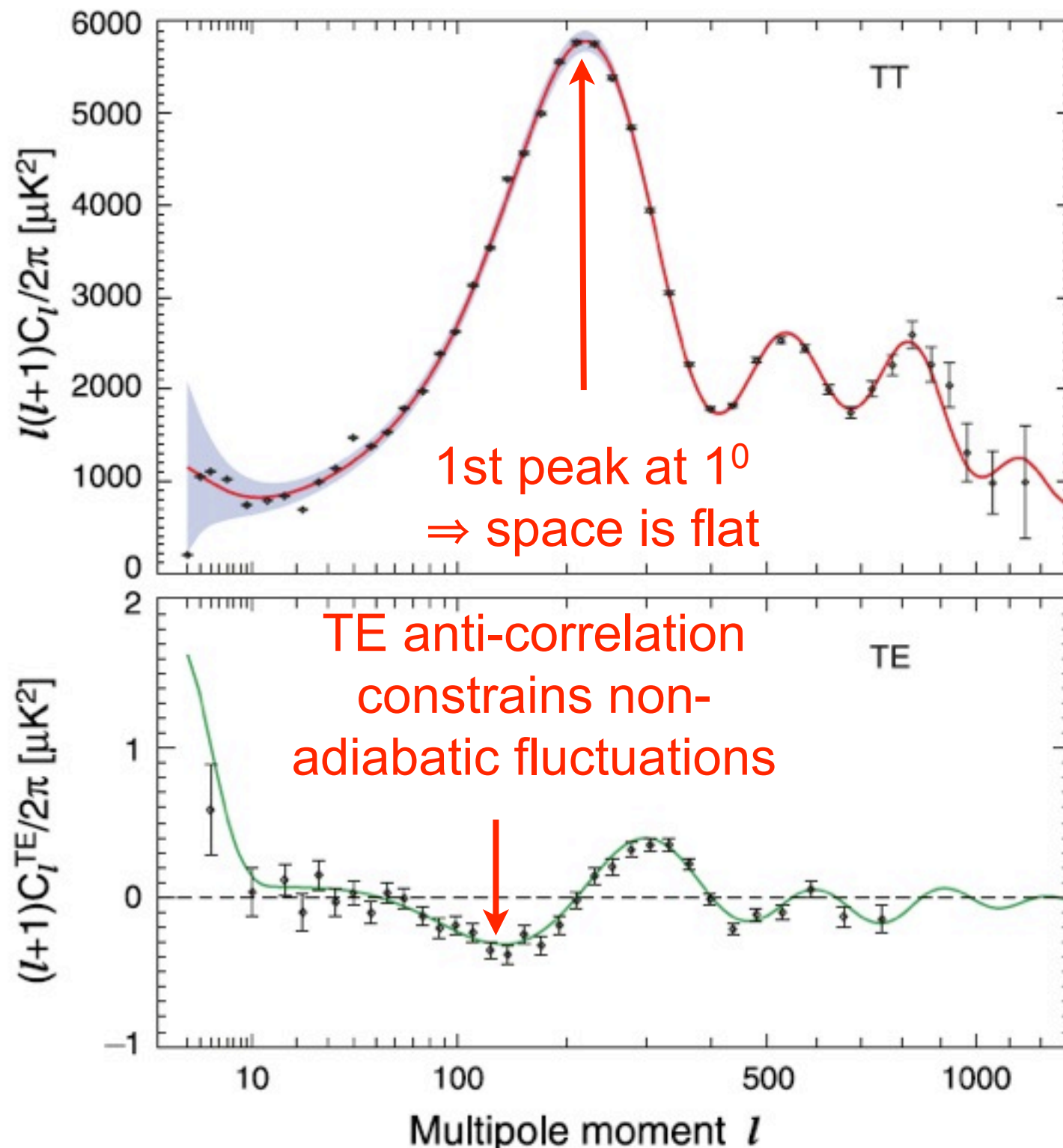TE anti-correlation constrains non-adiabatic fluctuations

Fig. 9.— The temperature (TT) and temperature-polarization (TE) power spectra for the seven-year WMAP data set. The solid lines show the predicted spectrum for the best-fit flat ΛCDM model. The error bars on the data points represent measurement errors while the shaded region indicates the uncertainty in the model spectrum arising from cosmic variance.

Description	Symbol	WMAP-only	WMAP+BAO+H_0
Parameters for Standard ΛCDM Model [a]			
Age of universe	t_0	13.75 ± 0.13 Gyr	13.75 ± 0.11 Gyr
Hubble constant	H_0	71.0 ± 2.5 km/s/Mpc	$70.4^{+1.3}_{-1.4}$ km/s/Mpc
Baryon density	Ω_b	0.0449 ± 0.0028	0.0456 ± 0.0016
Physical baryon density	$\Omega_b h^2$	$0.02258^{+0.00057}_{-0.00056}$	0.02260 ± 0.00053
Dark matter density	Ω_c	0.222 ± 0.026	0.227 ± 0.014
Physical dark matter density	$\Omega_c h^2$	0.1109 ± 0.0056	0.1123 ± 0.0035
Dark energy density	Ω_Λ	0.734 ± 0.029	$0.728^{+0.015}_{-0.016}$
Curvature fluctuation amplitude, $k_0 = 0.002$ Mpc^{-1} [b]	$\Delta^2_\mathcal{R}$	$(2.43 \pm 0.11) \times 10^{-9}$	$(2.441^{+0.088}_{-0.092}) \times 10^{-9}$
Fluctuation amplitude at $8h^{-1}$ Mpc	σ_8	0.801 ± 0.030	0.809 ± 0.024
Scalar spectral index	n_s	0.963 ± 0.014	0.963 ± 0.012
Redshift of matter-radiation equality	z_{eq}	3196^{+134}_{-133}	3232 ± 87
Angular diameter distance to matter-radiation eq.[c]	$d_A(z_{eq})$	14281^{+158}_{-161} Mpc	14238^{+128}_{-129} Mpc
Redshift of decoupling	z_*	$1090.79^{+0.94}_{-0.92}$	$1090.89^{+0.68}_{-0.69}$
Age at decoupling	t_*	379164^{+5187}_{-5243} yr	377730^{+3205}_{-3200} yr
Angular diameter distance to decoupling [c,d]	$d_A(z_*)$	14116^{+160}_{-163} Mpc	14073^{+129}_{-130} Mpc
Sound horizon at decoupling [d]	$r_s(z_*)$	$146.6^{+1.5}_{-1.6}$ Mpc	146.2 ± 1.1 Mpc
Acoustic scale at decoupling [d]	$l_A(z_*)$	302.44 ± 0.80	302.40 ± 0.73
Reionization optical depth	τ	0.088 ± 0.015	0.087 ± 0.014
Redshift of reionization	z_{reion}	10.5 ± 1.2	10.4 ± 1.2
Parameters for Extended Models [e]			
Total density [f]	Ω_{tot}	$1.080^{+0.093}_{-0.071}$	$1.0023^{+0.0056}_{-0.0054}$
Equation of state [g]	w	$-1.12^{+0.42}_{-0.43}$	-0.980 ± 0.053
Tensor to scalar ratio, $k_0 = 0.002$ Mpc^{-1} [b,h]	r	< 0.36 (95% CL)	< 0.24 (95% CL)
Running of spectral index, $k_0 = 0.002$ Mpc^{-1} [b,i]	$dn_s/d\ln k$	-0.034 ± 0.026	-0.022 ± 0.020
Neutrino density [j]	$\Omega_\nu h^2$	< 0.014 (95% CL)	< 0.0062 (95% CL)
Neutrino mass [j]	$\sum m_\nu$	< 1.3 eV (95% CL)	< 0.58 eV (95% CL)
Number of light neutrino families [k]	N_{eff}	> 2.7 (95% CL)	$4.34^{+0.86}_{-0.88}$

N. Jarosik et al. - January 2010

Table 8. WMAP Seven-year Cosmological Parameter Summary

The parameters reported in the first section assume the 6 parameter flat CDM model, first using WMAP data only (Larson et al. 2010), **then using WMAP+BAO+H0 data** (Komatsu et al. 2010). The H0 data consists of a Gaussian prior on the present-day value of the Hubble constant, H0 = 74.2±3.6 km s−1 Mpc−1(Riess et al. 2009), while the BAO priors on the distance ratio rs(zd)/Dv(z) at z = 0.2, 0.3 are obtained from the Sloan Digital Sky Survey Data Release 7 (Percival et al. 2009). **Uncertainties are 68% CL unless otherwise noted.**

SEVEN-YEAR WILKINSON MICROWAVE ANISOTROPY PROBE (WMAP) OBSERVATIONS: COSMOLOGICAL INTERPRETATION - E. Komatsu, et al. - January 2010

The combination of 7-year data from *WMAP* and improved astrophysical data rigorously tests the standard cosmological model and places new constraints on its basic parameters and extensions. By combining the *WMAP* data with the latest distance measurements from the Baryon Acoustic Oscillations (BAO) in the distribution of galaxies (Percival et al. 2009) and the Hubble constant (H_0) measurement (Riess et al. 2009), we determine the parameters of the simplest 6-parameter ΛCDM model. The power-law index of the primordial power spectrum is $n_s = 0.963 \pm 0.012$ (68% CL) for this data combination, a measurement that excludes the Harrison-Zel'dovich-Peebles spectrum by more than 3σ. The other parameters, including those beyond the minimal set, are also consistent with, and improved from, the 5-year results. We find no convincing deviations from the minimal model. The 7-year temperature power spectrum gives a better determination of the third acoustic peak, which results in a better determination of the redshift of the matter-radiation equality epoch. Notable examples of improved parameters are the total mass of neutrinos, $\sum m_\nu < 0.58$ eV (95% CL), and the effective number of neutrino species, $N_{\text{eff}} = 4.34^{+0.86}_{-0.88}$ (68% CL), which benefit from better determinations of the third peak and H_0. The limit on a constant dark energy equation of state parameter from *WMAP*+BAO+H_0, without high-redshift Type Ia supernovae, is $w = -1.10 \pm 0.14$ (68% CL). We detect the effect of primordial helium on the temperature power spectrum and provide a new test of big bang nucleosynthesis by measuring $Y_p = 0.326 \pm 0.075$ (68% CL). We detect, and show on the map for the first time, the tangential and radial polarization patterns around hot and cold spots of temperature fluctuations, an important test of physical processes at $z = 1090$ and the dominance of adiabatic scalar fluctuations. The 7-year polarization data have significantly improved: we now detect the temperature-E-mode polarization cross power spectrum at 21σ, compared to 13σ from the 5-year data. With the 7-year temperature-B-mode cross power spectrum, the limit on a rotation of the polarization plane due to potential parity-violating effects has improved by 38% to $\Delta\alpha = -1.1° \pm 1.3°$ (statistical) $\pm 1.5°$ (systematic) (68% CL). We report a significant (8σ) detection of the Sunyaev-Zel'dovich (SZ) effect at the locations of known clusters of galaxies, and show that the measured SZ signal is a factor of 0.5 to 0.7 times the predictions from analytical models, hydrodynamical simulations, and X-ray observations. This lower amplitude is consistent with the lower-than-expected SZ power spectrum recently measured by the South Pole Telescope collaboration.

SEVEN-YEAR WILKINSON MICROWAVE ANISOTROPY PROBE (WMAP) OBSERVATIONS: COSMOLOGICAL INTERPRETATION - E. Komatsu, et al. - January 2010

TABLE 1
SUMMARY OF THE COSMOLOGICAL PARAMETERS OF ΛCDM MODEL

Class	Parameter	WMAP 7-year ML[a]	WMAP+BAO+H_0 ML	WMAP 7-year Mean[b]	WMAP+BAO+H_0 Mean
Primary	$100\Omega_b h^2$	2.270	2.246	$2.258^{+0.057}_{-0.056}$	2.260 ± 0.053
	$\Omega_c h^2$	0.1107	0.1120	0.1109 ± 0.0056	0.1123 ± 0.0035
	Ω_Λ	0.738	0.728	0.734 ± 0.029	$0.728^{+0.015}_{-0.016}$
	n_s	0.969	0.961	0.963 ± 0.014	0.963 ± 0.012
	τ	0.086	0.087	0.088 ± 0.015	0.087 ± 0.014
	$\Delta^2_\mathcal{R}(k_0)$[c]	2.38×10^{-9}	2.45×10^{-9}	$(2.43 \pm 0.11) \times 10^{-9}$	$(2.441^{+0.088}_{-0.092}) \times 10^{-9}$
Derived	σ_8	0.803	0.807	0.801 ± 0.030	0.809 ± 0.024
	H_0	71.4 km/s/Mpc	70.2 km/s/Mpc	71.0 ± 2.5 km/s/Mpc	$70.4^{+1.3}_{-1.4}$ km/s/Mpc
	Ω_b	0.0445	0.0455	0.0449 ± 0.0028	0.0456 ± 0.0016
	Ω_c	0.217	0.227	0.222 ± 0.026	0.227 ± 0.014
	$\Omega_m h^2$	0.1334	0.1344	$0.1334^{+0.0056}_{-0.0055}$	0.1349 ± 0.0036
	z_{reion}[d]	10.3	10.5	10.5 ± 1.2	10.4 ± 1.2
	t_0[e]	13.71 Gyr	13.78 Gyr	13.75 ± 0.13 Gyr	13.75 ± 0.11 Gyr

[a] Larson et al. (2010). "ML" refers to the Maximum Likelihood parameters.

[b] Larson et al. (2010). "Mean" refers to the mean of the posterior distribution of each parameter. The quoted errors show the 68% confidence levels (CL).

[c] $\Delta^2_\mathcal{R}(k) = k^3 P_\mathcal{R}(k)/(2\pi^2)$ and $k_0 = 0.002$ Mpc^{-1}.

[d] "Redshift of reionization," if the universe was reionized instantaneously from the neutral state to the fully ionized state at z_{reion}. Note that these values are somewhat different from those in Table 1 of Komatsu et al. (2009b), largely because of the changes in the treatment of reionization history in the Boltzmann code CAMB (Lewis 2008).

[e] The present-day age of the universe.

The constraint on N_{eff} can also be interpreted as an upper bound on the energy density in primordial gravitational waves with frequencies $> 10^{-15}$ Hz. Many cosmological mechanisms for the generation of stochastic gravitational waves exist, such as certain inflationary models, electroweak phase transitions, and cosmic strings.

With the current WMAP+BAO+H_0 data combination, we define $N_{\text{gw}} = N_{\text{eff}} - 3.04$, and find limits of

$$N_{\text{gw}} < 2.85, \quad \Omega_{\text{gw}} h^2 < 1.60 \times 10^{-5} \text{ (95\%CL)}$$

for adiabatic initial conditions, imposing an $N_{\text{eff}} \geq 3.04$ prior.

Late Cosmological Epochs
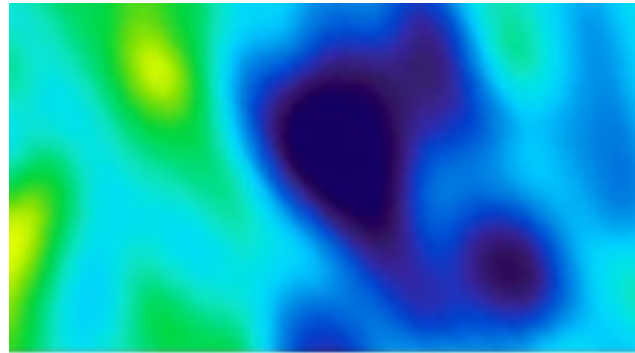
380 kyr   z~1000

recombination
last scattering

dark ages

~100 Myr   z~30

first stars
"reionization"

~480 Myr z~10

galaxy formation

13.7 Gyr   z=0

today

Gravitational instability

small-amplitude fluctuations:

$\bar{\rho}$
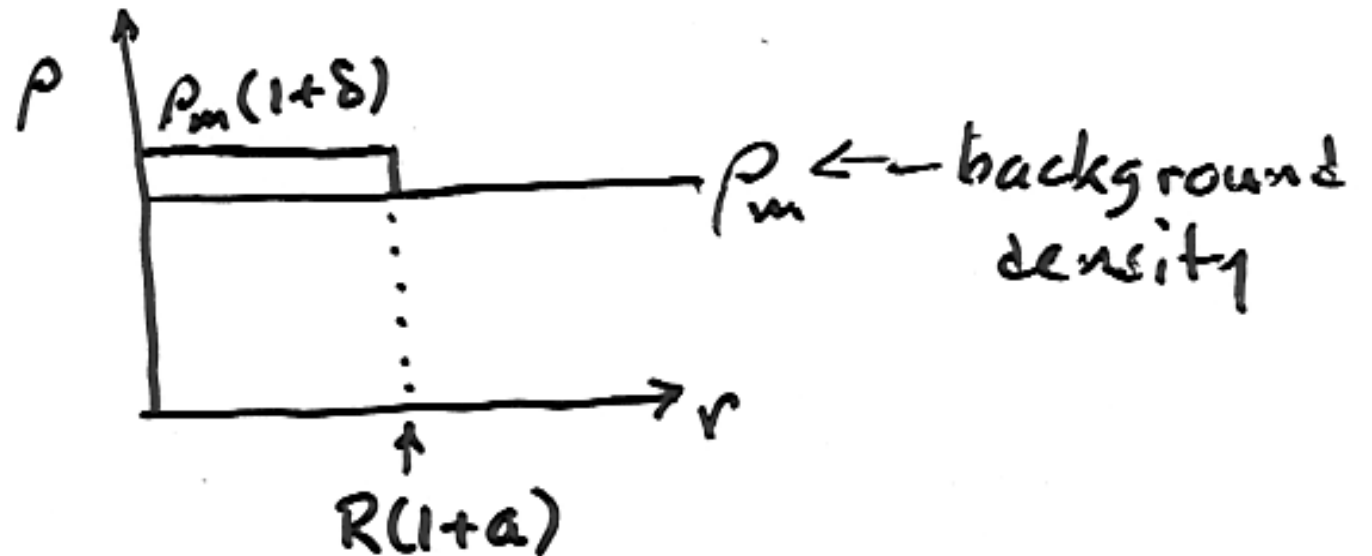
gravitational instability:

galaxy   cluster

$\bar{\rho}$

void

0
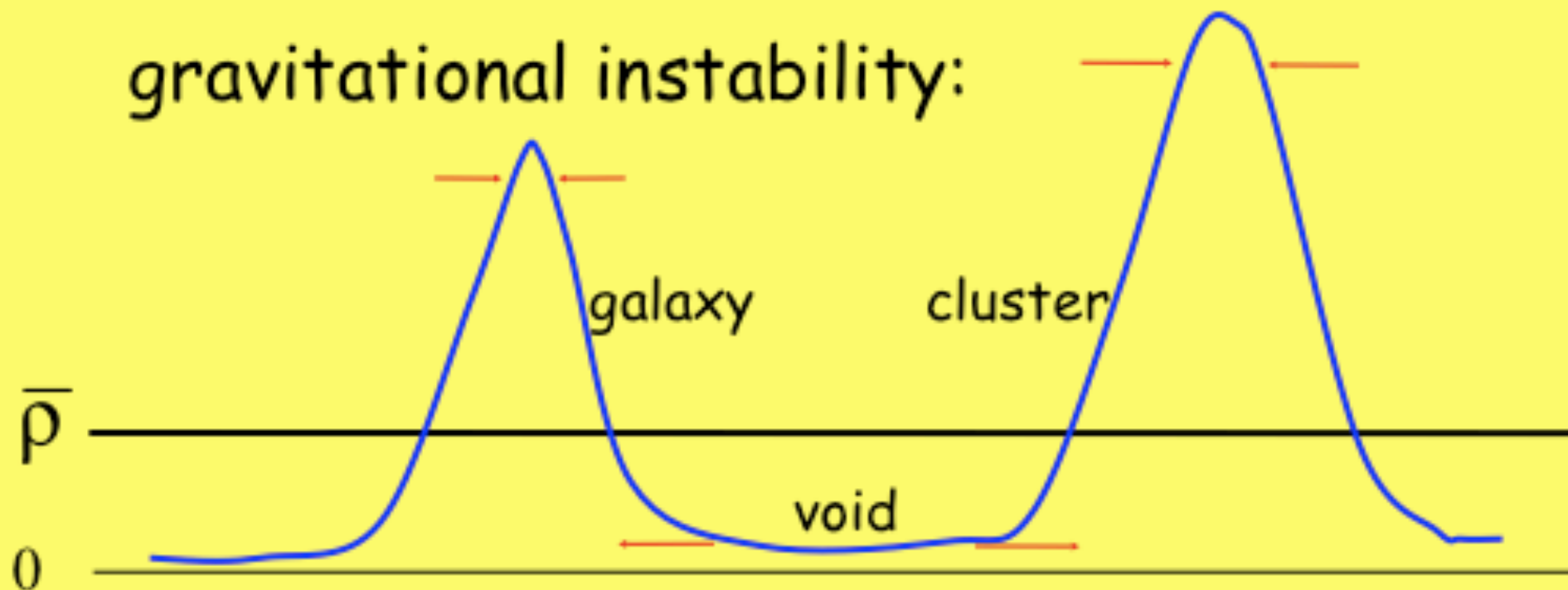
FLUCTUATIONS: LINEAR THEORY

Recall: $E(ii) - E(00) \Rightarrow \dfrac{2\ddot{a}}{a} = -\dfrac{8\pi}{3}G\rho - 8\pi Gp + \dfrac{2}{3}\Lambda$ (here a = R, Λ=0)

"TOP HAT MODEL"

MASS CONS. $\Rightarrow$

$\rho_m (1+\delta) R^3 (1+a)^3 = const. \Rightarrow$

$\delta = -3a$

GRAVITY: $\ddot{R} = -\dfrac{4\pi G}{3}(\rho + 3p)R$

$$\boxed{\ddot{\delta} + 2\dfrac{\dot{R}}{R}\dot{\delta} = 4\pi G \rho_m \delta}$$

RAD ERA $\dot{R}/R = \dfrac{1}{2} t^{-1}$,

MATTER ERA $= \dfrac{2}{3} t^{-1}$,
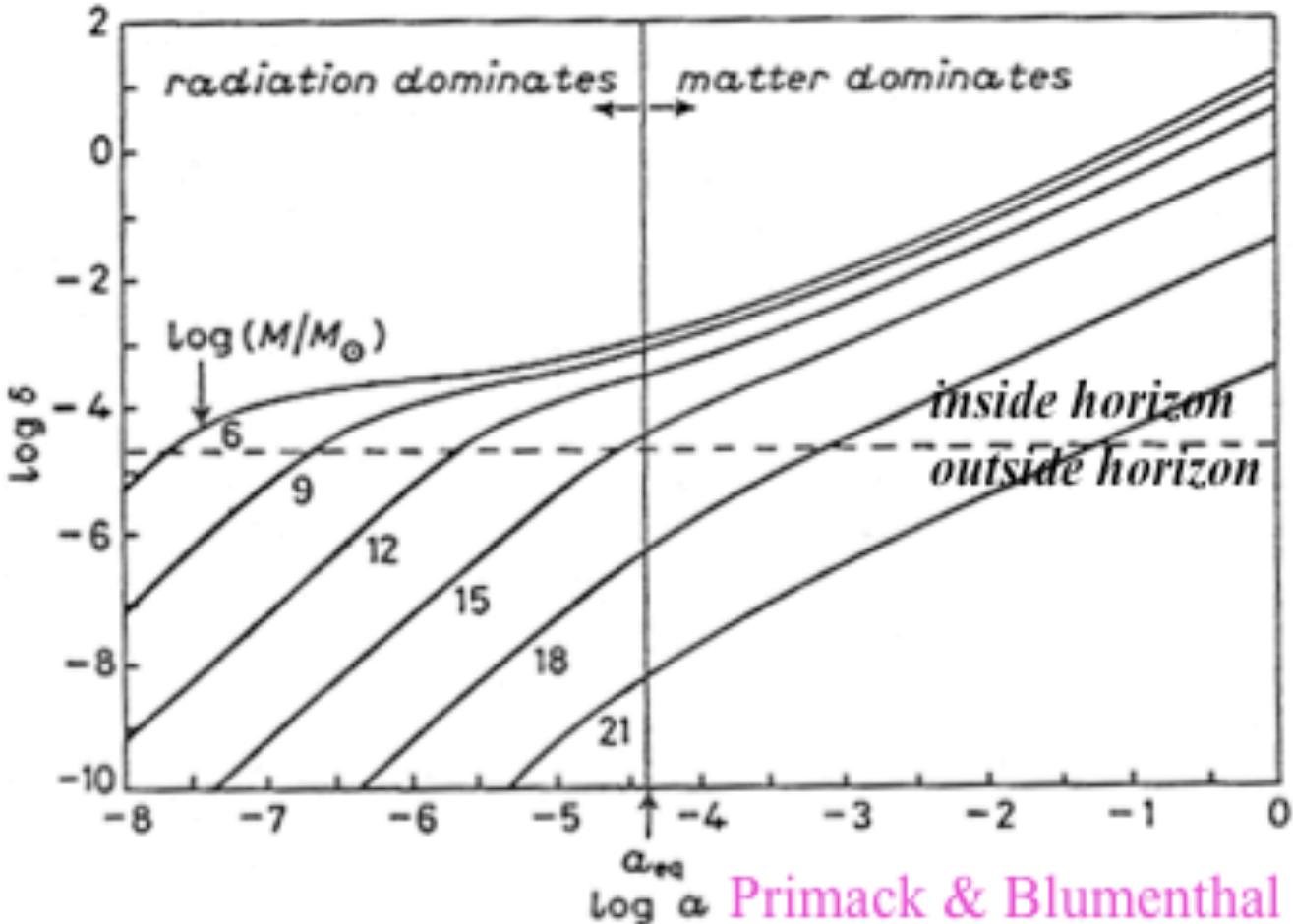
APPLIED BOTH TO FLUCT. + BCG. $\Rightarrow$

Try $\delta = t^{\alpha}$

$\delta = At + Bt^{-1} = \underline{AR^2} + BR^{-2}$

$\delta = At^{2/3} + Bt^{-1} = \underline{AR} + BR^{-3/2}$

GROWING MODE

CDM Structure Formation: Linear Theory

Primack & Blumenthal 1983

Cluster and smaller-scale ν fluctuations damp because of "free-streaming"

Matter fluctuations that enter the horizon during the radiation dominated era, with masses less than about $10^{15} M_\odot$, grow only $\propto \log a$, because they are not in the gravitationally dominant component. But matter fluctuations that enter the horizon in the matter-dominated era grow $\propto a$. This explains the characteristic shape of the CDM fluctuation spectrum, with $\delta(k) \propto k^{-n/2-2} \log k$ for $k \gg k_{eq}$.
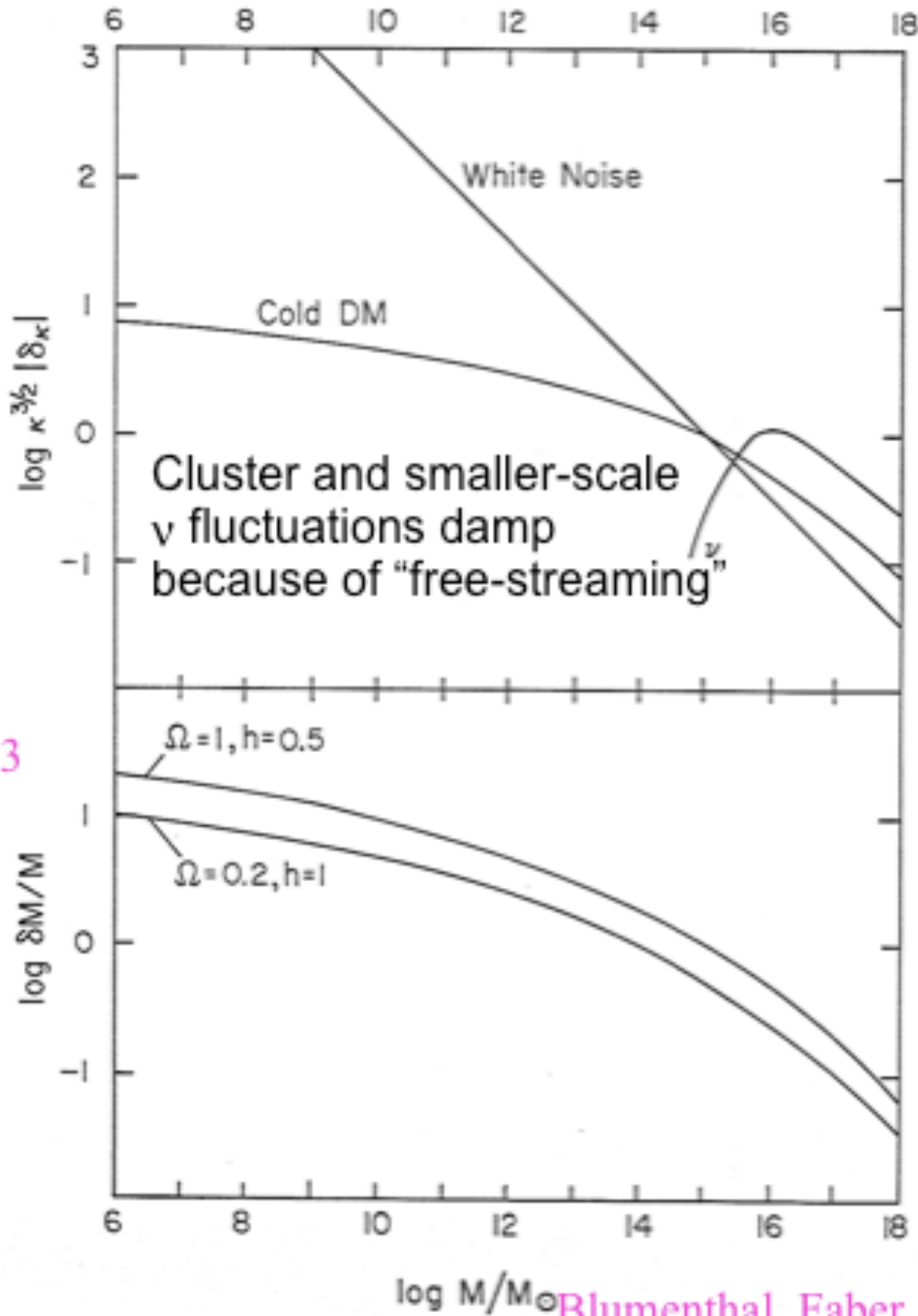
Blumenthal, Faber, Primack, & Rees 1984

The Initial Fluctuations

At Inflation: Gaussian, adiabatic

Fourier transform:

$$\delta(\vec{x}) = \sum_{k} \delta_{\vec{k}} \, e^{i\vec{k}\cdot\vec{x}}$$

Power Spectrum:

$$P(k) \equiv \,<|\,\widetilde{\delta}(\vec{k})|^2> \, \propto k^n$$

rms perturbation:

$$\delta_{rms} = \,<\delta^2>^{1/2} \, \propto \int_{k=0}^{k_{max}} P_k \, d^3k \quad \propto M^{-(n+3)/6}$$

Correlation function:

$$\xi(r) \equiv \,<\delta(\vec{x})\delta(\vec{x}+\vec{r})> \, \propto \int |\,\widetilde{\delta}(\vec{k})|^2 \, e^{-i\vec{k}\cdot\vec{r}} d^3k \, \propto r^{-(n+3)}$$

$$dP = [1+\xi(r)]\,n\,dV$$

Gravitational Instability: Dark Matter

Small fluctuations: $\delta, v, \varphi \quad (x, t)$ comoving coordinates

$r = a(t)x$ etc.

$H \equiv \dot{a}/a, \quad \Omega(t)$

matter era

Continuity: $\dot{\delta} + \nabla \times v + \nabla \cdot (v\delta) = 0$

Euler: $\dot{v} + 2Hv + (v \times \nabla)v = -\nabla\varphi$

Poisson: $\nabla^2\varphi = (3/2)H^2\Omega\delta$

Linear approximation: $\ddot{\delta} + 2H\dot{\delta} = (3/2)H^2\Omega\delta$

growing mode: $\delta \propto D(t) = t^{2/3} \xrightarrow[\Omega_m \to 0]{} t^0$

$\delta = -\nabla \cdot v / [Hf(\Omega)]$ $f(\Omega) \equiv \dot{D}/(HD) \approx \Omega^{0.6}$

irrotational, potential flow: $\nabla \times v = 0$ $v = -\nabla\varphi_v$

Thus far, we have considered only the evolution of fluctuations in the dark matter. But of course we have to consider also the ordinary matter, known in cosmology as "baryons" (implicitly including the electrons). See Madau's lectures "The Astrophysics of Early Galaxy Formation" (http://arxiv.org/abs/0706.0123v1) for a summary. We have already seen that the baryons are primarily in the form of atoms after $z \sim 1000$, with a residual ionization fraction of a few x 10^{-4}. They become fully reionized by $z \sim 6$, but they were not reionized at $z \sim 20$ since the COBE satellite found that "Compton parameter" $y \leq 1.5$ x 10^{-5}, where

$$y = \int_0^z \frac{k_B T_e}{m_e c^2} \frac{d\tau_e}{dz} dz \quad \text{with} \quad (n_e \sigma_T c dt) = d\tau_e \, , \quad \sigma_T = (8\pi/3)(e^2/mc^2)^2$$

This implies that $\quad \langle x_e T_e \rangle [(1+z)^{3/2} - 1] < 4 \times 10^7 \text{ K.}$ Thus, for example, a universe that was reionized and reheated at $z = 20$ to $(x_e, T_e) = (1, > 4 \times 10^5 \text{ K})$ would violate the COBE y-limit.

The figure at right shows the evolution of the radiation (dashed line, labeled CMB) and matter (solid line, labeled GAS) temperatures after recombination, in the absence of any reheating mechanism.
(From Madau's lectures, at physics.ucsc.edu/~joel/Phys224 .)
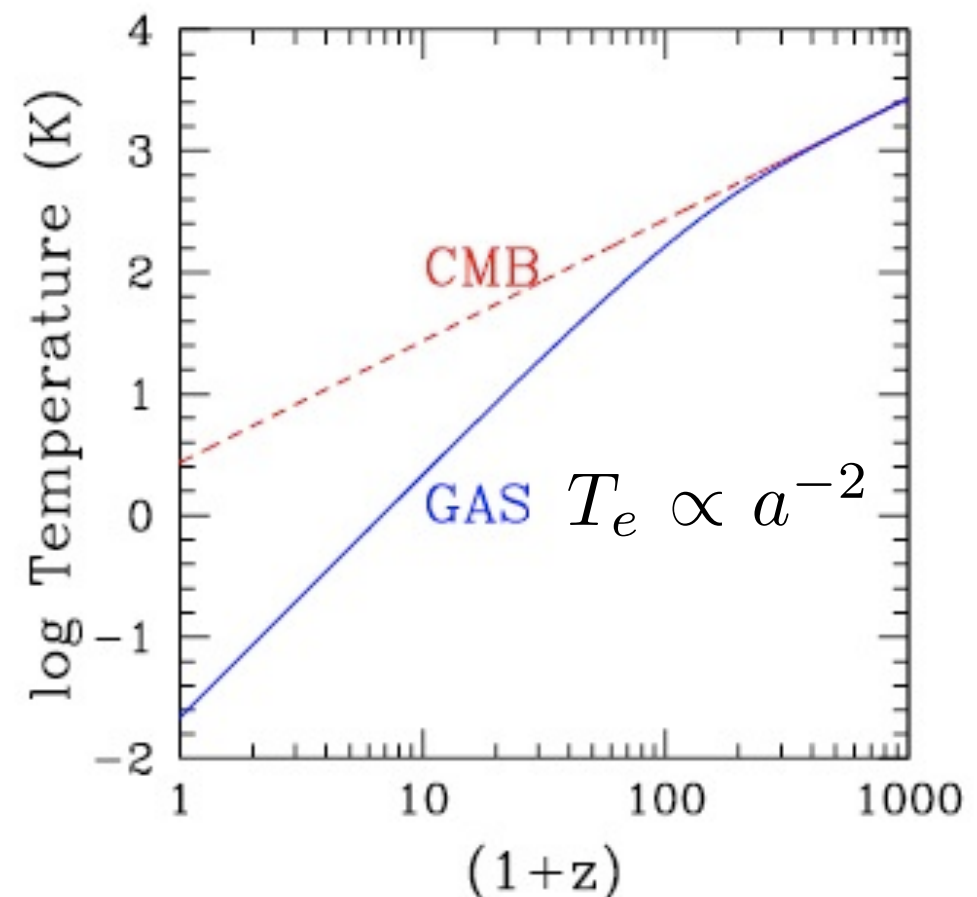
The linear evolution of sub-horizon density perturbations in the dark matter-baryon fluid is governed in the matter-dominated era by two second-order differential equations:

$$\ddot{\delta}_{\mathrm{dm}} + 2H\dot{\delta}_{\mathrm{dm}} = \frac{3}{2}H^2\Omega_m^z\left(f_{\mathrm{dm}}\delta_{\mathrm{dm}} + f_b\delta_b\right) \tag{1}$$

for the dark matter, and   "Hubble friction"

$$\ddot{\delta}_b + 2H\dot{\delta}_b = \frac{3}{2}H^2\Omega_m^z\left(f_{\mathrm{dm}}\delta_{\mathrm{dm}} + f_b\delta_b\right) - \frac{c_s^2}{a^2}k^2\delta_b$$

for the baryons, where $\delta_{\mathrm{dm}}(k)$ and $\delta_b(k)$ are the Fourier components of the density fluctuations in the dark matter and baryons,† f_{dm} and f_b are the corresponding mass fractions, c_s is the gas sound speed, k is the (comoving) wavenumber, and the derivatives are taken with respect to cosmic time. Here

$$\Omega_m^z \equiv 8\pi G\rho(t)/3H^2 = \Omega_m(1+z)^3/[\Omega_m(1+z)^3 + \Omega_\Lambda] \tag{2}$$

is the time-dependent matter density parameter, and $\rho(t)$ is the total background matter density. Because there is ~5 times more dark matter than baryons, it is the former that defines the pattern of gravitational wells in which structure formation occurs. In the case where $f_b \approx 0$ and the universe is static ($H = 0$), equation (1) above becomes

---

† For each fluid component (i = b, dm) the real space fluctuation in the density field, $\delta_i(\mathbf{x}) \equiv \delta\rho_i(\mathbf{x})/\rho_i$, can be written as a sum over Fourier modes, $\delta_i(\mathbf{x}) = \int d^3\mathbf{k}\,(2\pi)^{-3}\,\delta_i(\mathbf{k})\,\exp i\mathbf{k}\cdot\mathbf{x}$.

$$\ddot{\delta}_{\rm dm} = 4\pi G\rho\delta_{\rm dm} \equiv \frac{\delta_{\rm dm}}{t_{\rm dyn}^2},$$

where $t_{\rm dyn}$ denotes the dynamical timescale. This equation has the solution

$$\delta_{\rm dm} = A_1 \exp(t/t_{\rm dyn}) + A_2 \exp(-t/t_{\rm dyn}).$$

After a few dynamical times, only the exponentially growing term is significant: gravity tends to make small density fluctuations in a static pressureless medium grow exponentially with time. Sir James Jeans (1902) was the first to discuss this.

The additional term $\propto H\dot{\delta}_{\rm dm}$ present in an expanding universe can be thought as a "Hubble friction" term that acts to slow down the growth of density perturbations. Equation (1) admits the general solution for the growing mode:

$$\delta_{\rm dm}(a) = \frac{5\Omega_m}{2} H_0^2 H \int_0^a \frac{da'}{(\dot{a}')^3}, \tag{3}$$

so that an Einstein-de Sitter universe gives the familiar scaling $\delta_{\rm dm}(a) = a$ with coefficient unity. The right-hand side of equation (3) is called the linear growth factor $D(a) = D_+(a)$. Different values of Ω_m, Ω_Λ lead to different linear growth factors.

Growing modes actually decrease in density, but not as fast as the average universe. Note how, in contrast to the exponential growth found in the static case, the growth of perturbations even in the case of an Einstein-de Sitter ($\Omega_m = 1$) universe is just algebraic rather than exponential. This was discovered by the Russian physicist Lifshitz (1946).

Since cosmological curvature is at most marginally important at the present epoch, it was negligible during the radiation-dominated era and at least the beginning of the matter-dominated era. But for $k = -1$, i.e. $\Omega < 1$, the growth of δ slows for $(R/R_o) \gtrsim \Omega_o$, as gravity becomes less important and the universe begins to expand freely. To discuss this case, it is convenient to introduce the variable

$$x \equiv \Omega^{-1}(t) - 1 = (\Omega_o^{-1} - 1)R(t)/R_o. \tag{2.55}$$

(Note that $\Omega(t) \longrightarrow 1$ at early times.) The general solution in the matter-dominated era is then (Peebles, 1980, §11)

$$\delta = \tilde{A}D_1(t) + \tilde{B}D_2(t), \tag{2.56}$$

where the growing solution is

$$D_1 = 1 + \frac{3}{x} + \frac{3(1+x)^{1/2}}{x^{3/2}} \ln\left[(1+x)^{1/2} - x^{1/2}\right] \tag{2.57}$$

and the decaying solution is

$$D_2 = (1+x)^{1/2}/x^{3/2}. \tag{2.58}$$

These agree with the Einstein-de Sitter results (2.53) at early times ($t \ll t_o, x \ll 1$). For late times ($t \gg t_o, x \gg 1$) the solutions approach

$$D_1 = 1, D_2 = x^{-1}; \tag{2.59}$$

in this limit the universe is expanding freely and the amplitude of fluctuations stops growing.

The consequence is that dark matter fluctuations grow proportionally to the scale factor a(t) when matter is the dominant component of the universe, but only logarithmically when radiation is dominant. Thus there is not much difference in the amplitudes of fluctuations of mass $M < 10^{15}$ M_{sun}, which enter the horizon before $z_{mr} \sim 4 \times 10^3$, while there is a stronger dependance on M for fluctuations with $M > 10^{15}$ M_{sun}.
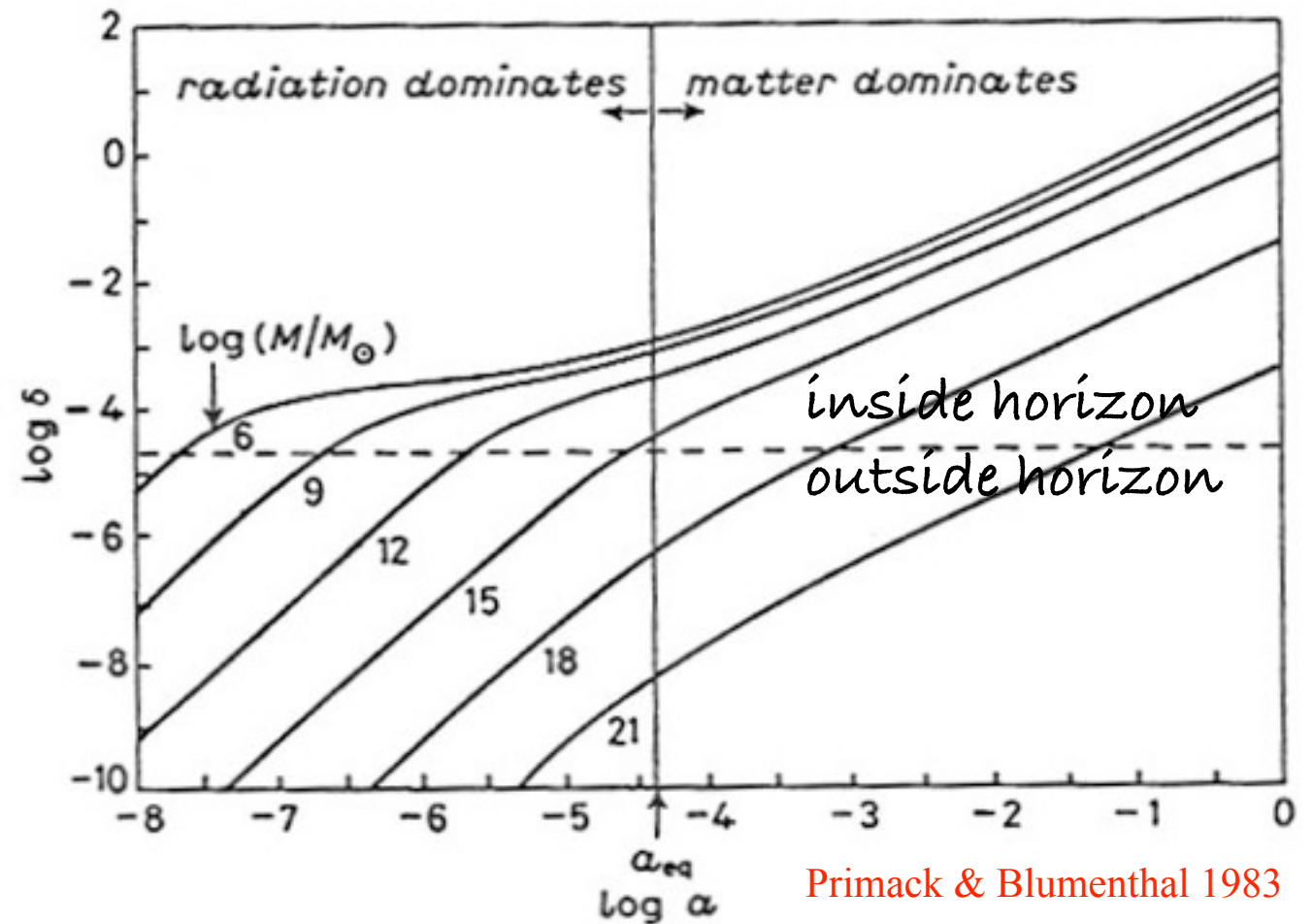
There is a similar suppression of the growth of matter fluctuations once the gravitationally dominant component of the universe is the dark energy, for example a cosmological constant. Lahav, Lilje, Primack, & Rees (1991) showed that the growth factor in this case is well approximated by

$$\delta_{\mathrm{dm}}(a) = D(a) \simeq \frac{5\Omega_m^z}{2(1+z)}\left[(\Omega_m^z)^{4/7} - \frac{(\Omega_m^z)^2}{140} + \frac{209}{140}\Omega_m^z + \frac{1}{70}\right]^{-1}.$$

Here Ω_m^z is again given by $\Omega_m^z \equiv 8\pi G\rho(t)/3H^2 = \Omega_m(1+z)^3/[\Omega_m(1+z)^3 + \Omega_\Lambda]$

The Linear Transfer Function T(k)

The observed uniformity of the CMB guarantees that density fluctuations must have been quite small at decoupling, implying that the evolution of the density contrast can be studied at $z \lesssim z_{\text{dec}}$ using linear theory, and each mode $\delta(k)$ evolves independently. The inflationary model predicts a scale-inv $\approx$ iant primordial power spectrum of density fluctuations $P(k) \equiv \langle |\delta(k)|^2 \rangle \propto k^n$, with $n = 1$ (the so-called Harrison-Zel'dovich spectrum). It is the index n that governs the balance between large and small-scale power. In the case of a Gaussian random field with zero mean, the power spectrum contains the complete statistical information about the density inhomogeneity. It is often more convenient to use the dimensionless quantity $\Delta_k^2 \equiv [k^3 P(k)/2\pi^2]$, which is the power per logarithmic interval in wavenumber k. In the matter-dominated epoch, this quantity retains its initial primordial shape ($\Delta_k^2 \propto k^{n+3}$) only on very large scales. Small wavelength modes enter the horizon earlier on and their growth is suppressed more severely during the radiation-dominated epoch: on small scales the amplitude of Δ_k^2 is essentially suppressed by four powers of k (from k^{n+3} to k^{n-1}). If $n = 1$, then small scales will have nearly the same power except for a weak, logarithmic dependence. Departures from the initially scale-free form are described by the transfer function $T(k)$, defined such that $T(0) = 1$:

$$P(k,z) = Ak^n \left[\frac{D(z)}{D(0)} \right]^2 T^2(k),$$

where A is the normalization.

An approximate fitting function for T(k) in a ΛCDM universe is (Bardeen et al. 1986)

$$T_k = \frac{\ln(1 + 2.34q)}{2.34q} \left[1 + 3.89q + (16.1q)^2 + (5.46q)^3 + (6.71q)^4\right]^{-1/4},$$

where (Sugayama 1995)

$$q \equiv \frac{k/\text{Mpc}^{-1}}{\Omega_m h^2 \exp(-\Omega_b - \Omega_b/\Omega_m)}.$$

For accurate work, for example for starting high-resolution N-body simulations, it is best to use instead of fitting functions the numerical output of highly accurate integration of the Boltzmann equations, for example from CMBFast, which is available at http://lambda.gsfc.nasa.gov/toolbox/ which points to http://lambda.gsfc.nasa.gov/toolbox/tb_cmbfast_ov.cfm

W e l c o m e to the CMBFAST Website!

This is the most extensively used code for computing cosmic microwave background anisotropy, polarization and matter power spectra. The code has been tested over a wide range of cosmological parameters. We are continuously testing and updating the code based on suggestions from the cosmological community. Do not hesitate to contact us if you have any questions or suggestions.

U. Seljak & M. Zaldarriaga

CMB Toolbox Overview

We provide links to a number of useful tools for CMB and Astronomy in general.

CMB Tools

- CMB Simulations - High-resolution, full-sky microwave temperature simulations including secondary anisotropies.

- Contributed Software is an archive at a LAMBDA partner site for tools built by members of the community.
- CMBFast - A tool that computes spectra for the cosmic background for a given set of CMB parameters. LAMBDA provides a web-based interface for this tool. Seljak and Zaldarriaga
- CAMB - Code for Anisotropies in the Microwave Background that computes spectra for a set of CMB parameters. LAMBDA provides a web-based interface for this tool. Lewis and Challinor
- CMBEASY - A C++ package, initially based on CMBFAST, now featuring a parameter likelihood package as well. Doran
- CMBview - A Mac OS X program for viewing HEALPix-format CMB data on an OpenGL-rendered sphere. Portsmouth
- COMBAT - A set of computational tools for CMB analysis. Borrill et al.
- CosmoMC - A Markov-Chain Monte-Carlo engine for exploring cosmological parameter space. Lewis and Bridle
- CosmoNet - Accelerated cosmological parameter estimation using Neural Networks.
- GLESP - Gauss-Legendre sky pixelization package. Doroshkevich, et al.
- GSM - Predicted all-sky maps at any frequency from 10 MHz to 100 GHz. de Oliveira-Costa.
- HEALPix - A spherical sky pixelization scheme. The Wilkinson Microwave Anisotropy Probe (WMAP) data skymap products are supplied in this form. Górski et al.
- IGLOO - A sky pixelization package. Crittenden and Turok
- MADCAP - Microwave Anisotropy Data Computational Analysis Package. Borrill et al.
- PICO - Integrates with CAMB and/or CosmoMC for cosmological parameter estimation using machine learning. Wandelt and Fendt
- RADPACK - Radical Compression Analysis Package. Knox
- RECFAST- Software to calculate the recombination history of the Universe. Seager, Sasselov, and Scott
- SkyViewer - A LAMBDA-developed OpenGL-based program to display HEALPix-based skymaps stored in FITS format files. Phillips
- SpiCE - Spatially Inhomogenous Correlation Estimator. Szapudi et al.
- WMAPViewer - A LAMBDA-developed web-based CMB map viewing tool using a technology similar to that found on maps.google.com. Phillips
- WOMBAT - Microwave foreground emission tools. Gawiser, Finkbeiner, Jaff et al.
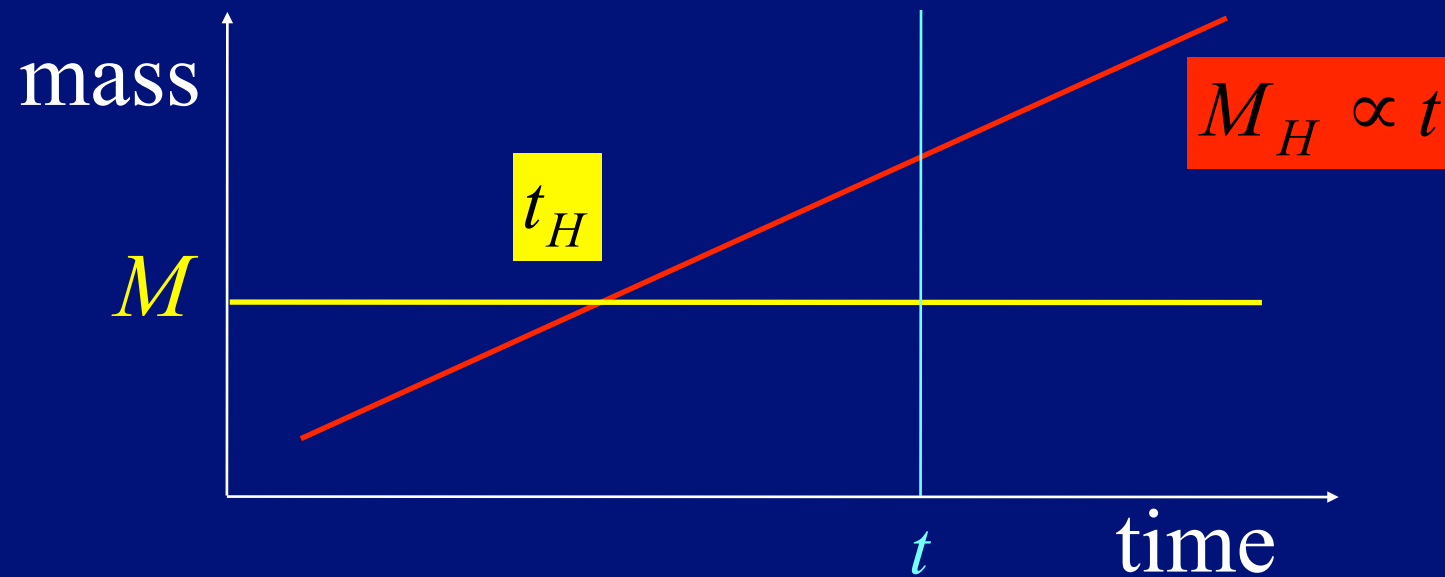
Likelihood Software

- SDSS LRG DR7 Likelihood Software - A software package that computes likelihoods for Luminous Red Galaxies (LRG) data from the seventh release of the Sloan Digital Sky Survey (SDSS).
- WMAP Likelihood Software - A software library used by the WMAP team to compute Fisher and Master matrices and to compute the likelihoods of various models. This is the same software found on the WMAP products list; more information may be found here.
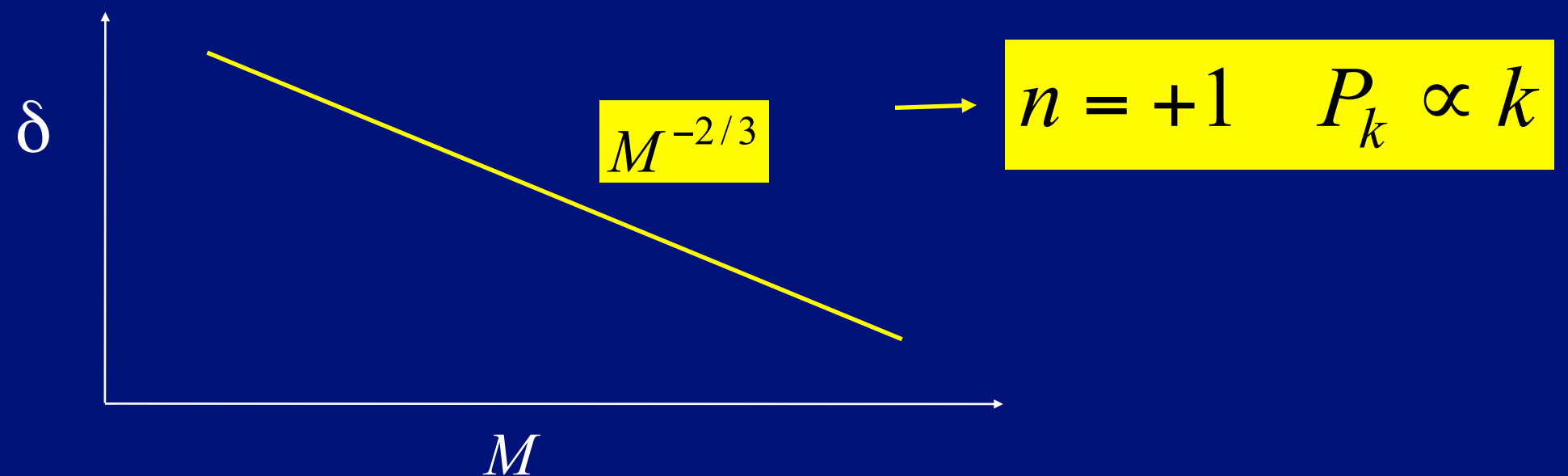
Other Tools

- WMAP Effective Frequency Calculator - A tool that calculates the effective frequencies of the five WMAP frequency bands.
- CFITSIO - A library of C and Fortran routines for reading and writing data in the FITS format.
- IDL Astro - The IDL Astronomy Users Library.
- Conversion Utilities - A small collection of astronomical conversion utilities.
- Calculators - A list of links to calculators.

This collection of tools can only be extended and improved with your input! Please feel free to send us suggestions and comments.
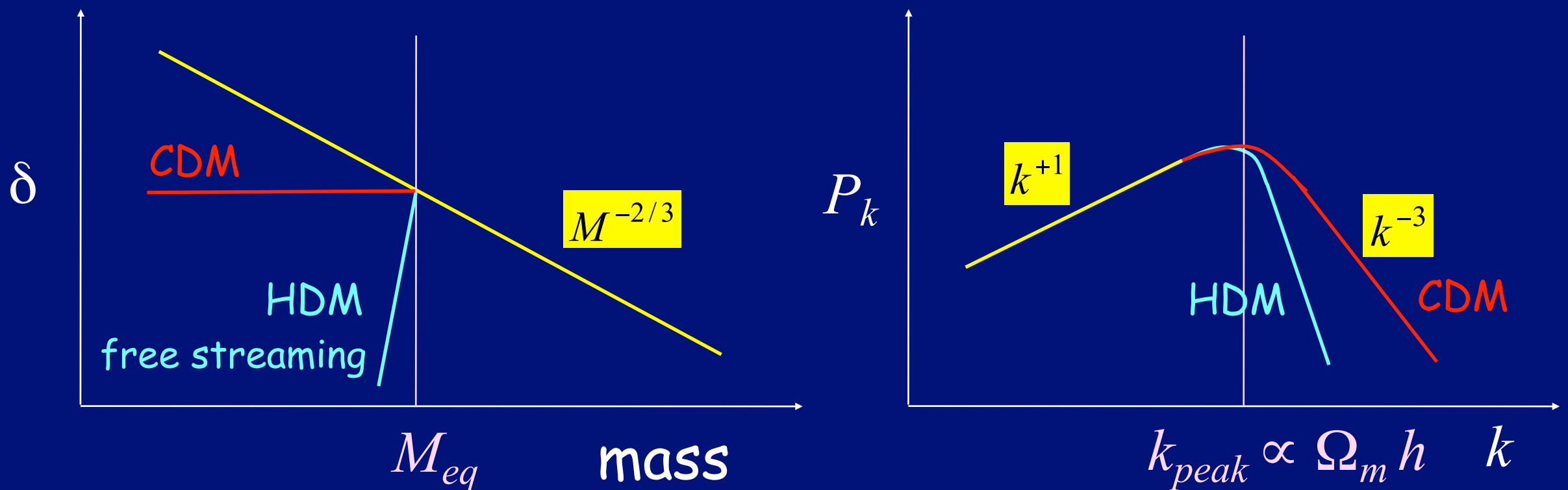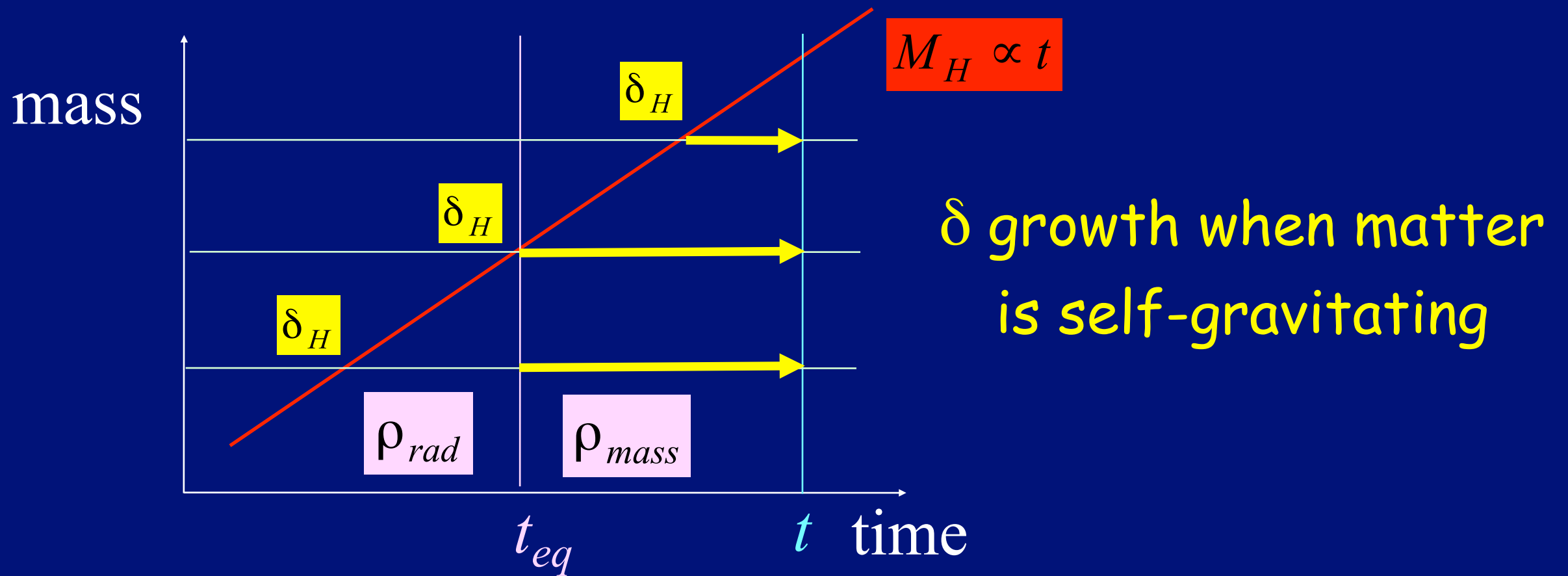
Thursday, May 3, 12

Scale-Invariant Spectrum (Harrison-Zel'dovich)

$$\delta(M,t) = \delta_H \left(\frac{t}{t_H(M)} \right)^{2/3} \propto M^{-2/3} t^{2/3}$$

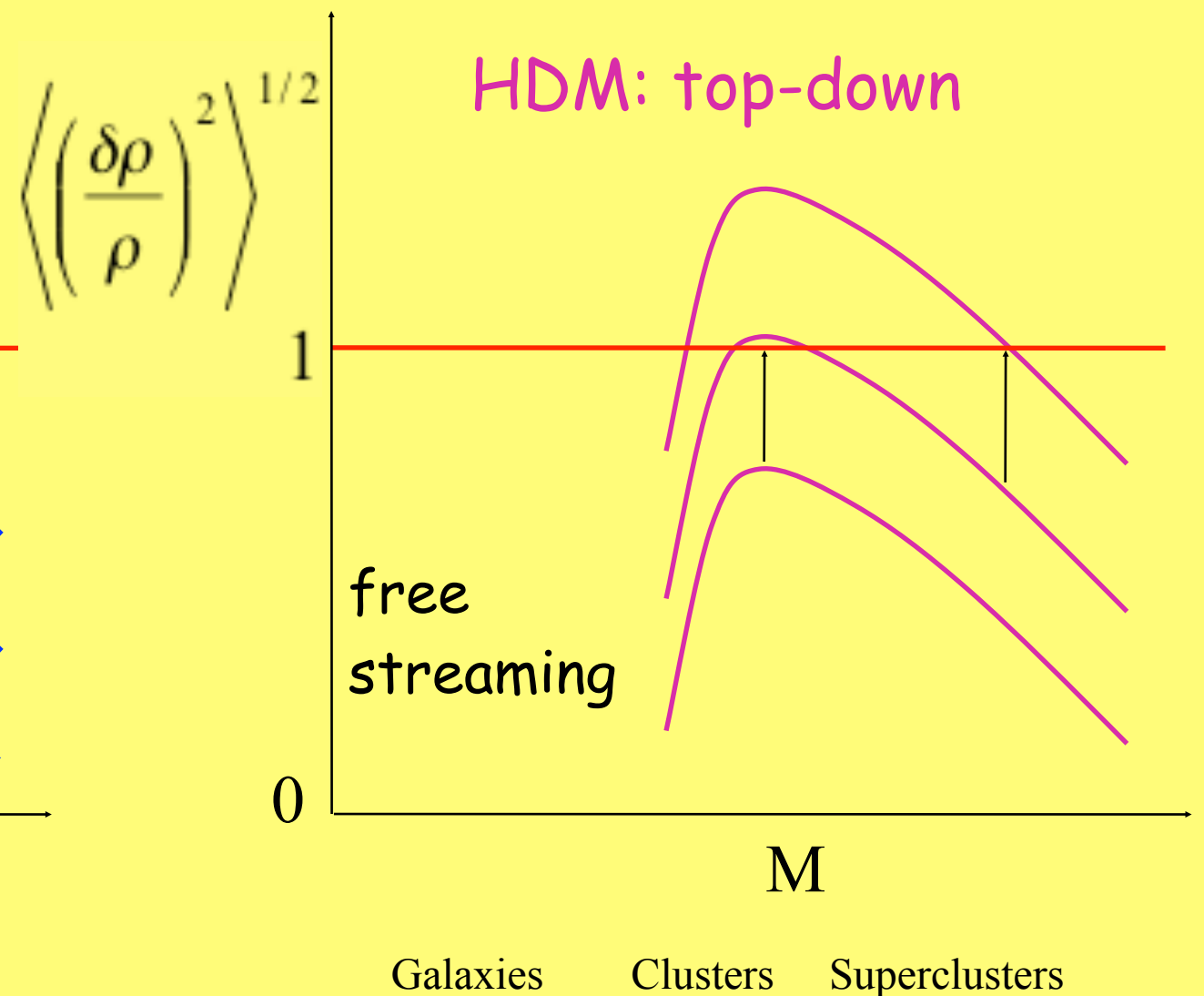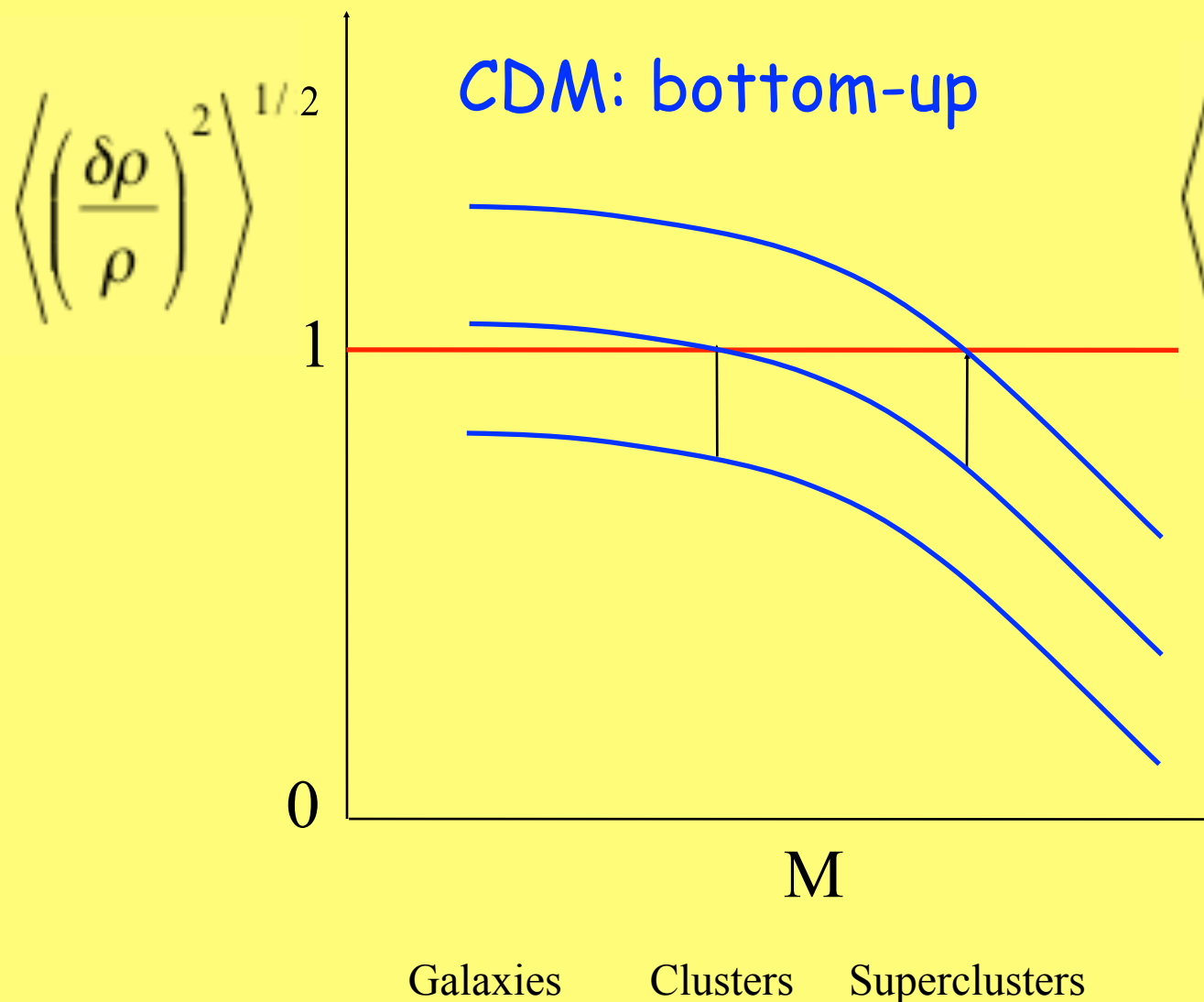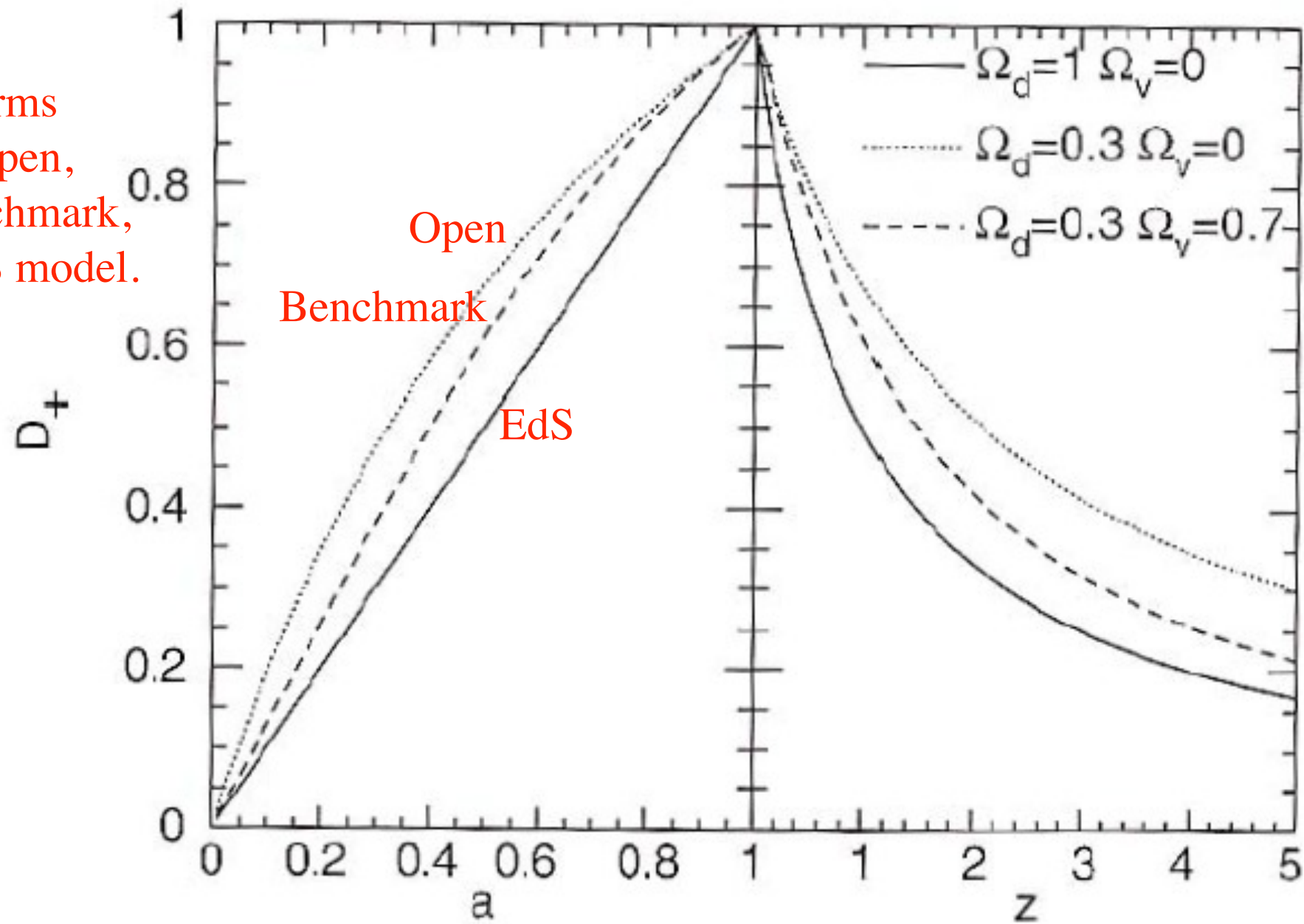$M_H \propto t$

$n = +1 \qquad P_k \propto k$

$M^{-2/3}$

CDM Power Spectrum

mass

$M_H \propto t$

δ_H

δ_H

δ_H

δ growth when matter is self-gravitating

ρ_{rad}

ρ_{mass}

t_{eq}

t time

δ

CDM

$M^{-2/3}$

HDM
free streaming

M_{eq} mass

P_k

k^{+1}

k^{-3}

HDM

CDM

$k_{peak} \propto \Omega_m h$ k

Formation of Large-Scale Structure

Fluctuation growth in the linear regime: $\delta \ll 1 \longrightarrow \delta \propto t^{2/3}$

rms fluctuation at mass scale M: $\delta \propto M^{-\alpha} \quad 0 < \alpha \leq 2/3$

CDM: bottom-up

$\left\langle \left(\dfrac{\delta\rho}{\rho}\right)^2 \right\rangle^{1/2}$

HDM: top-down

$\left\langle \left(\dfrac{\delta\rho}{\rho}\right)^2 \right\rangle^{1/2}$

free streaming

Galaxies   Clusters   Superclusters   Galaxies   Clusters   Superclusters

Structure forms earliest in Open, next in Benchmark, latest in EdS model.

$\Omega_d=1\ \Omega_v=0$ Einstein-de Sitter

$\Omega_d=0.3\ \Omega_v=0$ Open universe

$\Omega_d=0.3\ \Omega_v=0.7$ Benchmark model

Open

Benchmark

EdS

Fig. 7.3. Growth factor D_+ for three different cosmological models, as a function of the scale factor a (left panel) and of redshift (right panel). It is clearly visible how quickly D_+ decreases with increasing redshift in the EdS model, in comparison to the models of lower density

From Peter Schneider, *Extragalactic Astronomy and Cosmology* (Springer, 2006)

Thursday, May 3, 12

Linear Growth Rate Function $D(a)$

For completeness, here we present some approximations used in the text. For the family of flat cosmologies ($\Omega_m + \Omega_\Lambda = 1$) an accurate approximation for the value of the virial overdensity Δ_{vir} is given by the analytic formula (Bryan & Norman 1998):

$$\Delta_{\text{vir}} = (18\pi^2 + 82x - 39x^2)/\Omega(z), \tag{A1}$$

where $\Omega(z) \equiv \rho_m(z)/\rho_{\text{crit}}$ and $x \equiv \Omega(z) - 1$.

The linear growth-rate function $\delta(a)$, used in eqs. (14-15) and also in $\sigma_8(a)$ is defined as

$$\delta(a) = D(a)/D(1), \tag{A2}$$

where $a = 1/(1+z)$ is the expansion parameter and $D(a)$ is:

$$D(a) = \frac{5}{2}\left(\frac{\Omega_{m,0}}{\Omega_{\Lambda,0}}\right)^{1/3} \frac{\sqrt{1+x^3}}{x^{3/2}} \int_0^x \frac{x^{3/2}dx}{[1+x^3]^{3/2}}, \tag{A3}$$

$$x \equiv \left(\frac{\Omega_{\Lambda,0}}{\Omega_{m,0}}\right)^{1/3} a, \tag{A4}$$

where $\Omega_{m,0}$ and $\Omega_{\Lambda,0}$ are density contributions of matter and cosmological constant at $z = 0$. For $\Omega_m > 0.1$ the growth rate factor $D(a)$ can be accurately approximated by the following expressions (Lahav et al. 1991; Carroll et al. 1992):

$$D(a) = \frac{(5/2)a\Omega_m}{\Omega_m^{4/7} - \Omega_\Lambda + (1 + \Omega_m/2)(1 + \Omega_\Lambda/70)}, \tag{A5}$$

$$\Omega_m(a) = \Omega_{m,0}/(1+x^3), \tag{A6}$$

$$\Omega_\Lambda(a) = 1 - \Omega_m(a) \tag{A7}$$

For $\Omega_{m,0} = 0.27$ the error of these approximation is less than 7×10^{-4}.

Thursday, May 3, 12
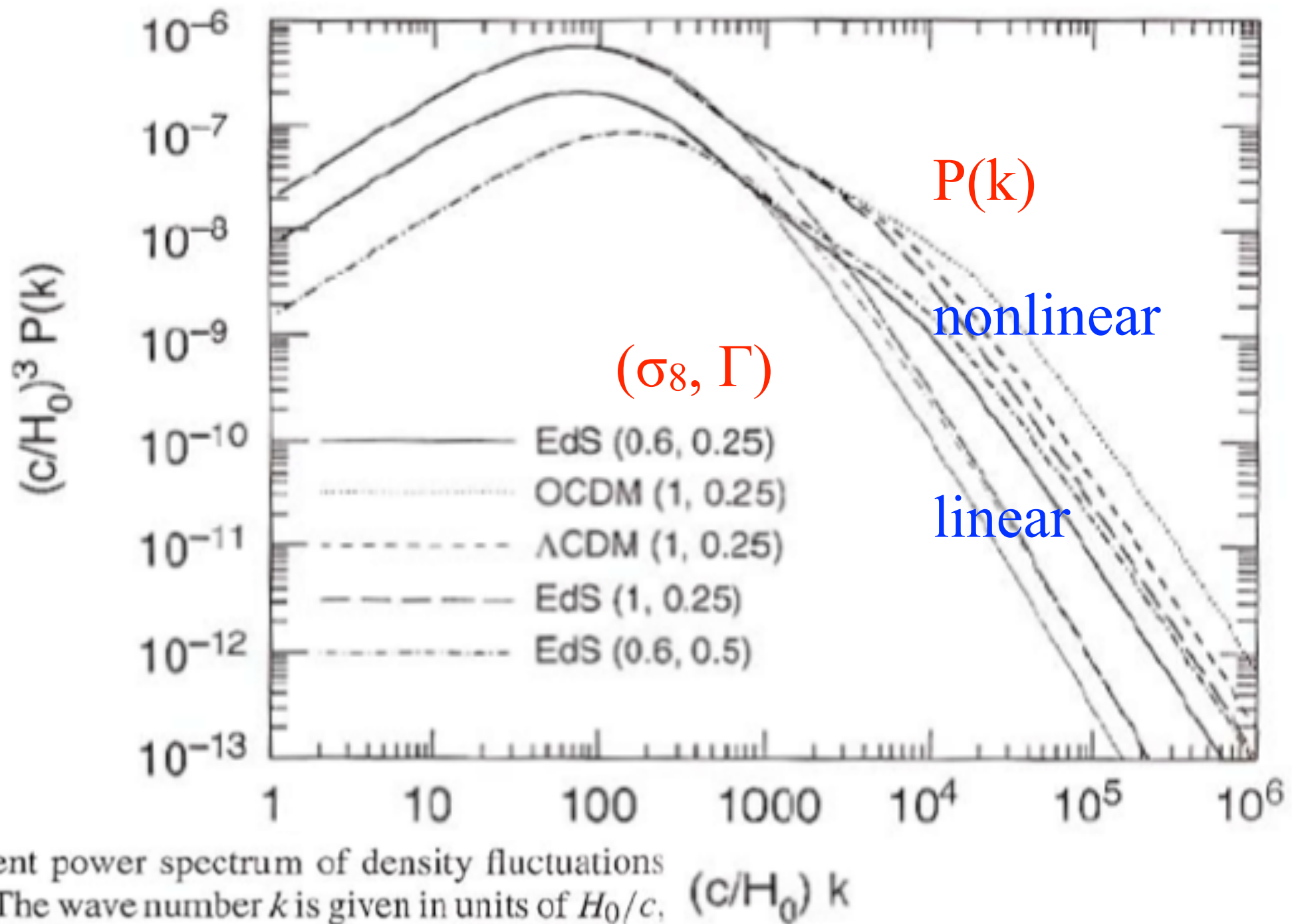
Fig. 7.6. The current power spectrum of density fluctuations for CDM models. The wave number k is given in units of H_0/c, and $(H_0/c)^3 P(k)$ is dimensionless. The various curves have different cosmological parameters: EdS: $\Omega_m = 1$, $\Omega_\Lambda = 0$; OCDM: $\Omega_m = 0.3$, $\Omega_\Lambda = 0$; ΛCDM: $\Omega_m = 0.3$, $\Omega_\Lambda = 0.7$. The values in parentheses specify (σ_8, Γ), where σ_8 is the normalization of the power spectrum (which will be discussed below), and where Γ is the shape parameter. The thin curves correspond to the power spectrum $P_0(k)$ linearly extrapolated to the present day, and the bold curves take the non-linear evolution into account

From Peter Schneider, *Extragalactic Astronomy and Cosmology* (Springer, 2006)

Thursday, May 3, 12

On large scales (k small), the gravity of the dark matter dominates. But on small scales, pressure dominates and growth of baryonic fluctuations is prevented. Gravity and pressure are equal at the Jeans scale

$$k_J = \frac{a}{c_s}\sqrt{4\pi G\rho}.$$

The Jeans mass is the dark matter + baryon mass enclosed within a sphere of radius $\pi a/k_J$,

$$M_J = \frac{4\pi}{3}\rho\left(\frac{\pi a}{k_J}\right)^3 = \frac{4\pi}{3}\rho\left(\frac{5\pi k_B T_e}{12G\rho m_p\mu}\right)^{3/2} \approx 8.8\times10^4\ \mathrm{M}_\odot\left(\frac{aT_e}{\mu}\right)^{3/2},$$

where μ is the mean molecular weight. The evolution of M_J is shown below, assuming that reionization occurs at $z=15$:
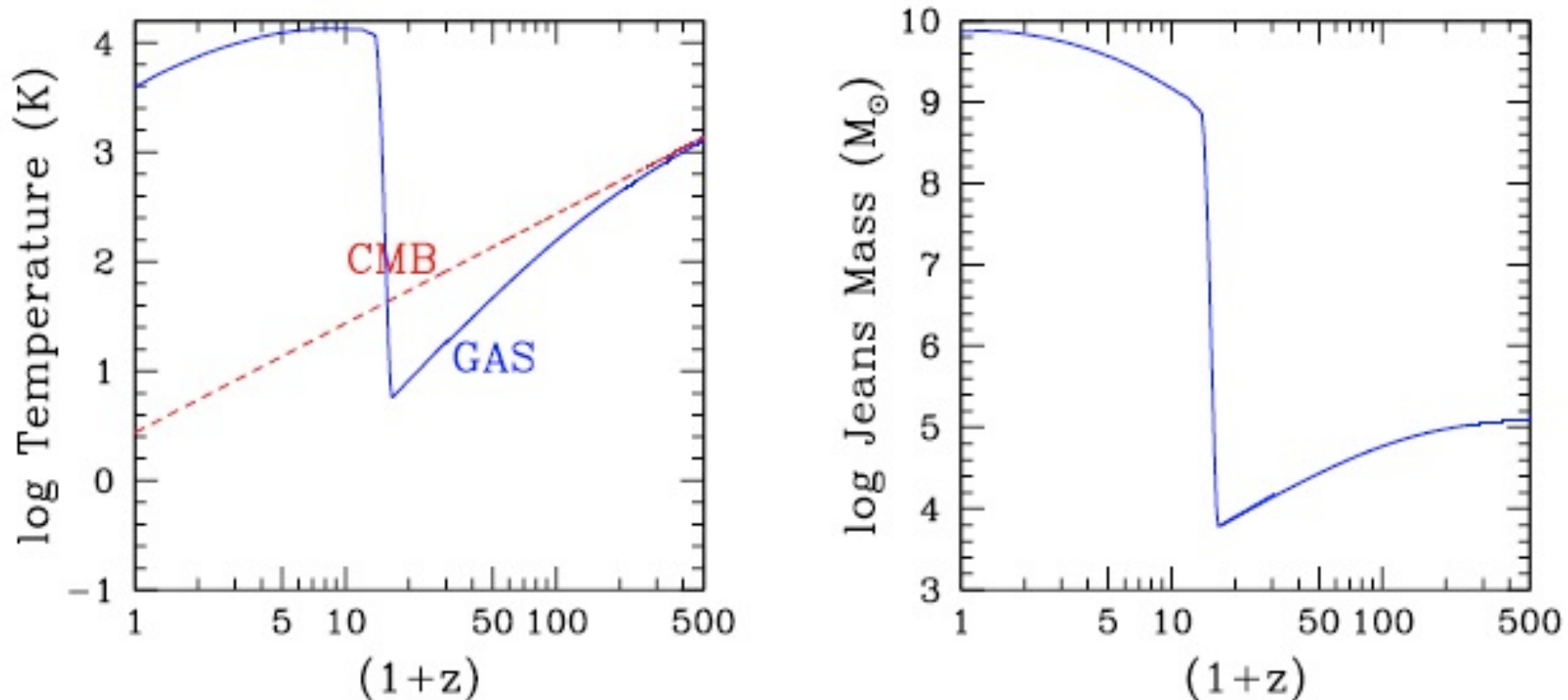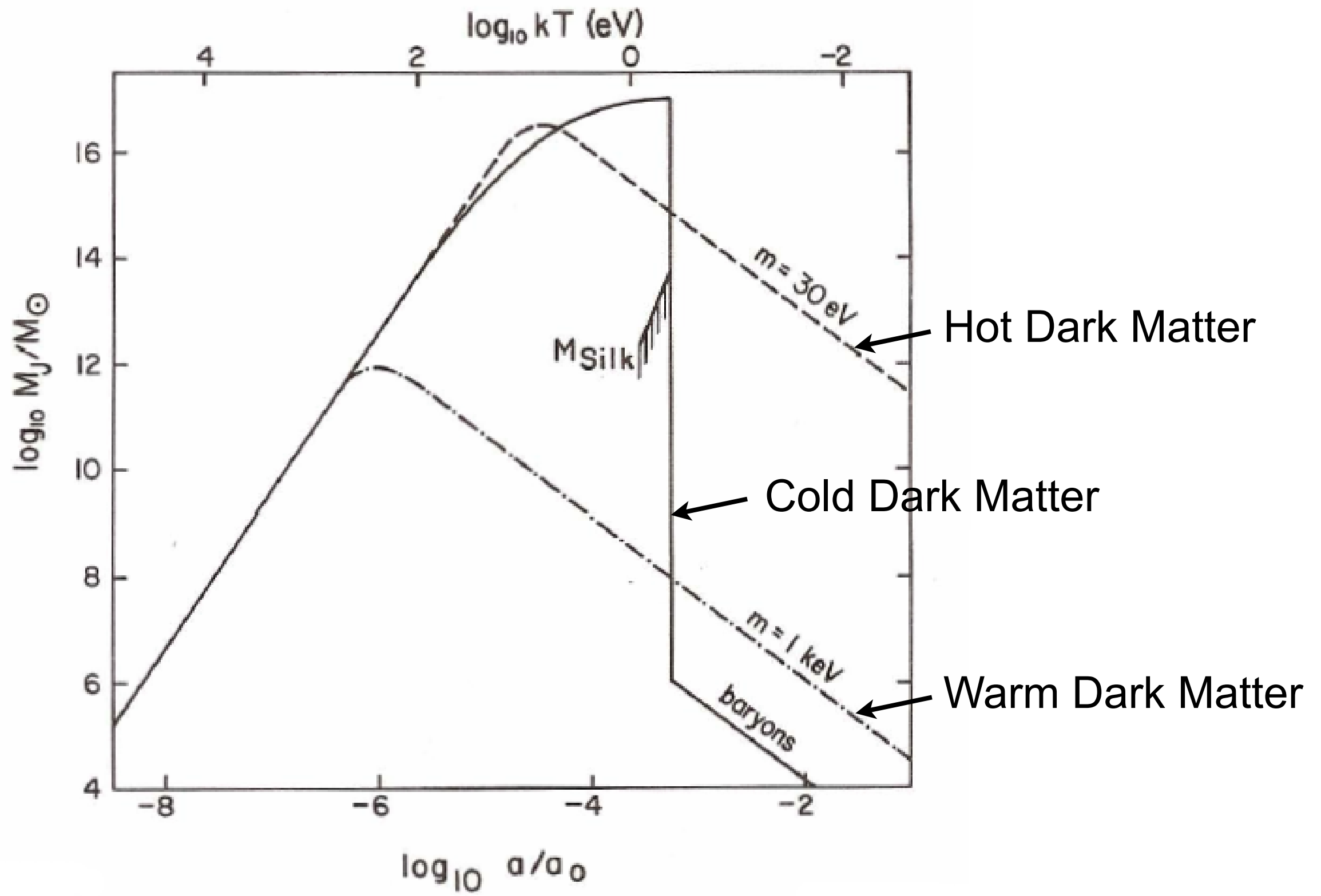
Jeans-type analysis for HDM, WDM, and CDM

GRAVITY – The Ultimate Capitalist Principle

Astronomers say that a region of the universe with more matter is "richer." Gravity magnifies differences—if one region is slightly denser than average, it will expand slightly more slowly and grow relatively denser than its surroundings, while regions with less than average density will become increasingly less dense. The rich always get richer, and the poor poorer.

Temperature map at 380,000 years after the Big Bang. **Blue** (cooler) regions are slightly denser. From NASA's **WMAP** satellite, 2003.
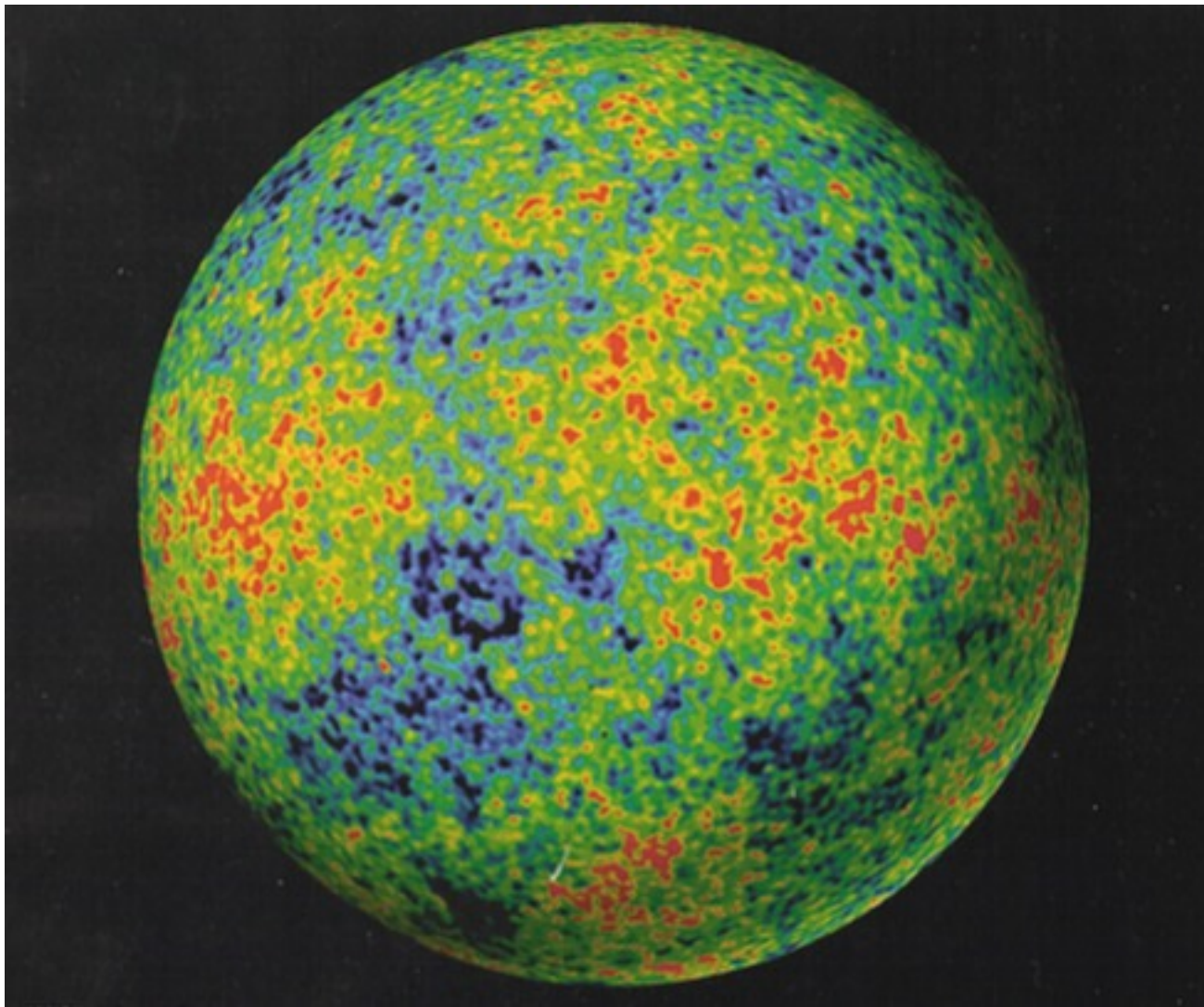
The early universe expands *almost* perfectly uniformly. But there are small differences in density from place to place (about 30 parts per million). Because of gravity, denser regions expand more slowly, less dense regions more rapidly. Thus gravity amplifies the contrast between them, until…

# Structure Formation by Gravitational Collapse
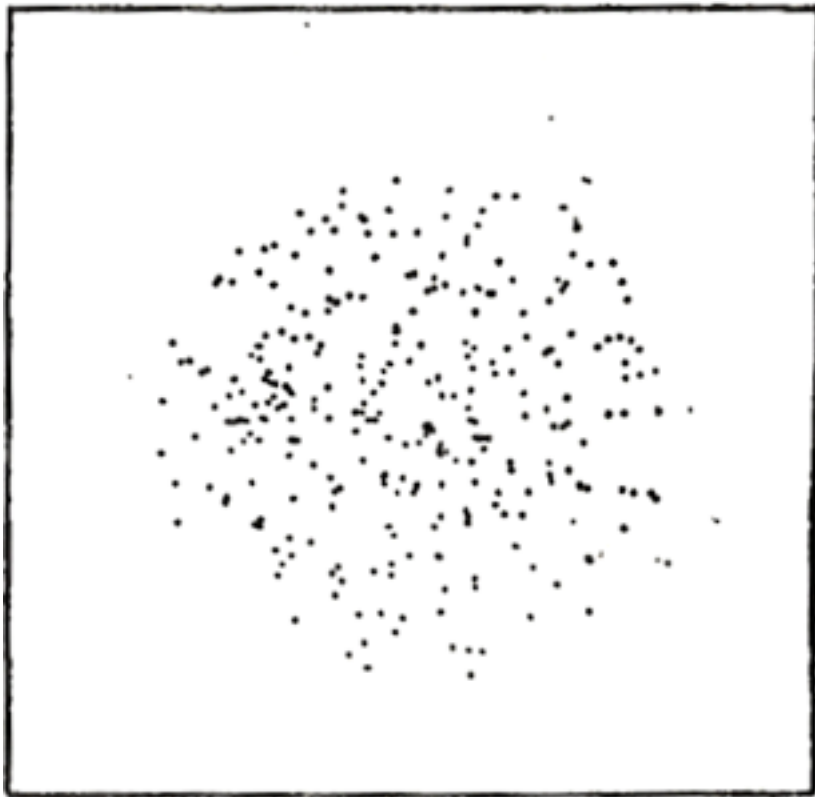
When any region becomes about twice as dense as typical regions its size, it reaches a maximum radius, **stops expanding,**

Simulation of top-hat collapse: P.J.E. Peebles 1970, ApJ, 75, 13.
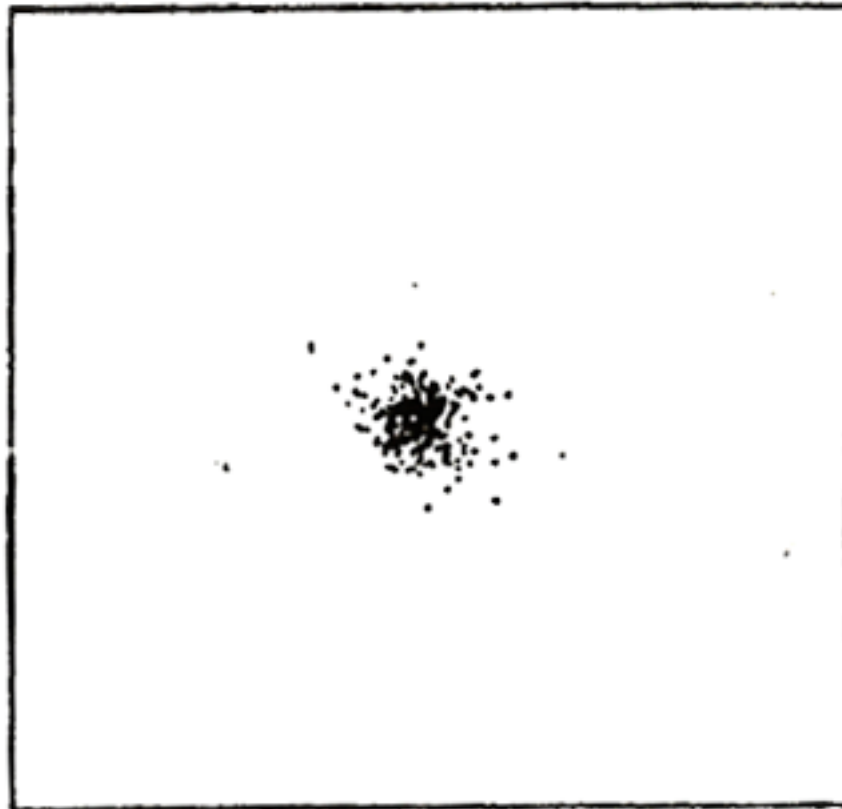
and starts falling together. The forces between the subregions generate velocities which **prevent** the material from **all falling toward the center**.

Used in my 1984 summer school lectures "Dark matter, Galaxies, and Large Scale Structure," http://tinyurl.com/3bjknb3
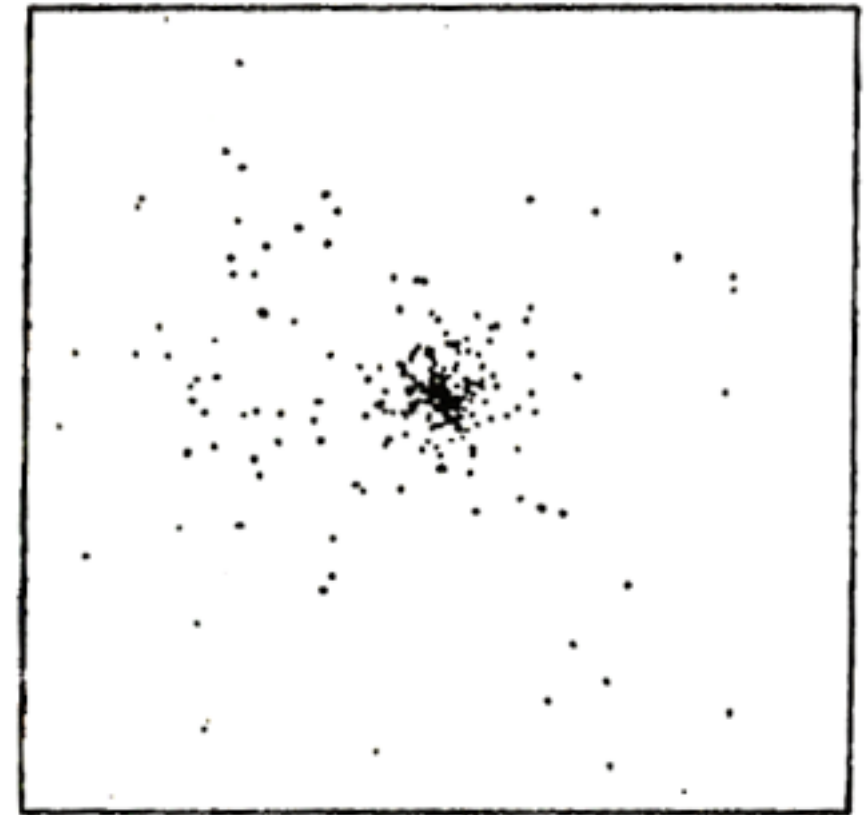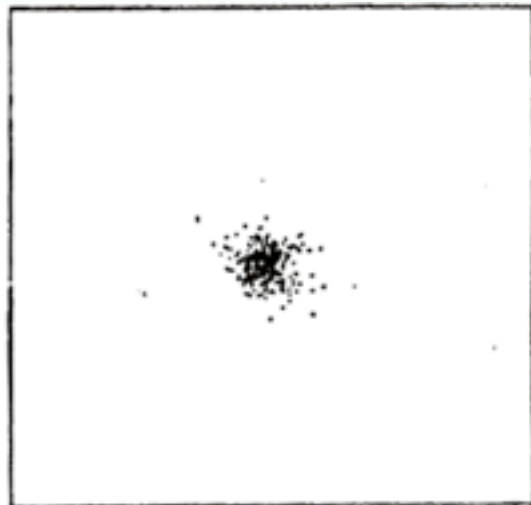
Through Violent Relaxation the dark matter quickly reaches a **stable configuration** that's about half the maximum radius but denser in the center.
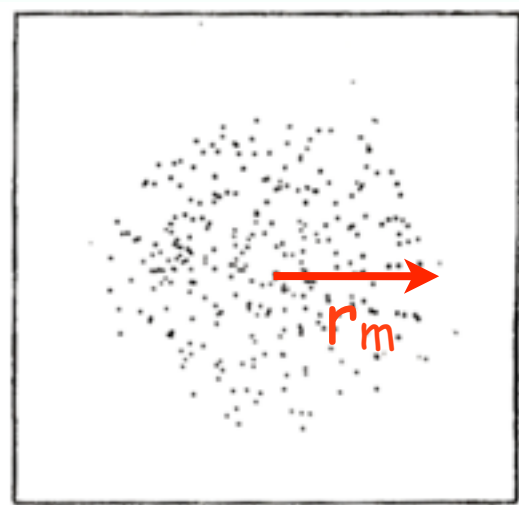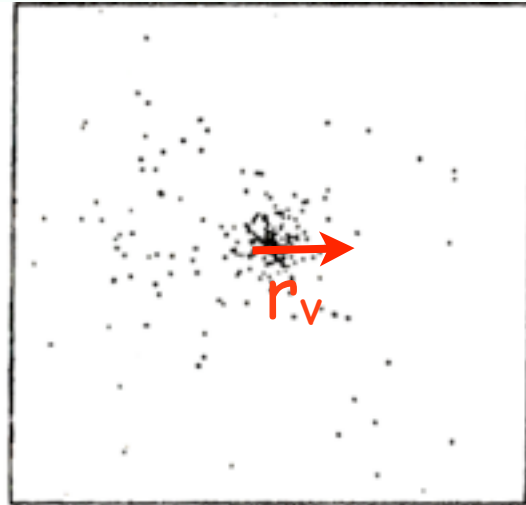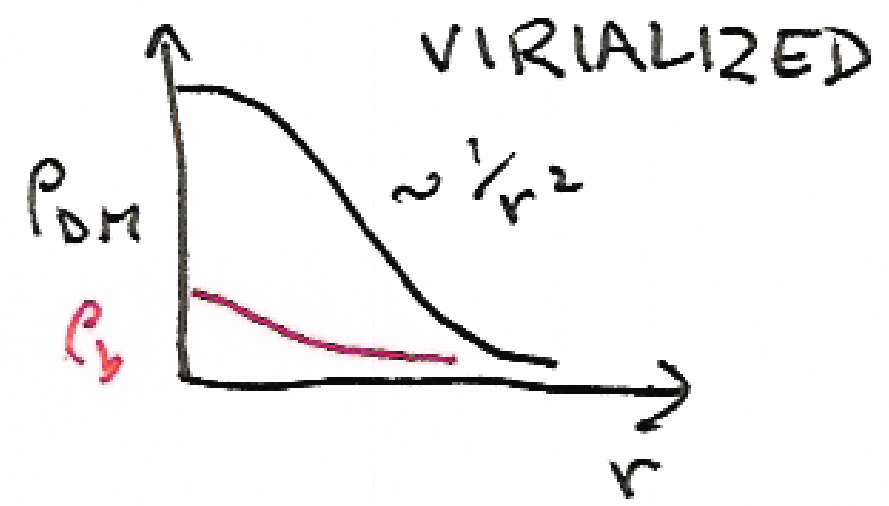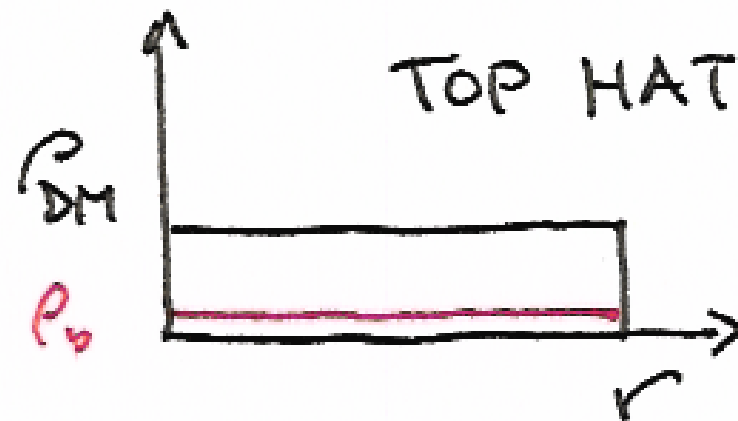
TOP HAT
Max Expansion

VIOLENT
RELAXATION

VIRIALIZED

Virial Theorem: $\langle K \rangle = -\frac{1}{2}\langle W \rangle$

$W_m = \frac{C}{r_m}$, so after virialization

$\frac{C}{r_m} = E = W + K = \frac{1}{2}\langle W \rangle = \frac{C}{2 r_G}$

$\Rightarrow r_v = \frac{1}{2} r_m$, $\rho_v = 8 \rho_m \approx 50 \bar{\rho}(t_m)$

$\langle v^2 \rangle \approx \frac{GM}{r_G}$

Growth and Collapse of Fluctuations

Schematic sketches of radius, density, and density contrast of an overdense fluctuation. It initially expands with the Hubble expansion, reaches a maximum radius (solid vertical line), and undergoes violent relaxation during collapse (dashed vertical line), which results in the dissipationless matter forming a stable halo. Meanwhile the ordinary matter ρb continues to dissipate kinetic energy and contract, thereby becoming more tightly bound, until dissipation is halted by star or disk formation, explaining the origin of galactic spheroids and disks.

(This was the simplified discussion of BFPR84; the figure is from my 1984 lectures at the Varenna school. Now we take into account halo growth by accretion, and the usual assumption is that spheroids form mostly as a result of galaxy mergers Toomre 1977.)